Zootaxa 2577: 1–45 (2010)
www.mapress.com/zootaxa/

Article

ISSN 1175-5326 (print edition)
ZOOTAXA
ISSN 1175-5334 (online edition)

New fossil mussels (Bivalvia: Mytilidae) from Miocene hydrocarbon seep deposits, North Island, New Zealand, with general remarks on vent and seep mussels

KRISTIAN P. SAETHER[1,5], CRISPIN T. S. LITTLE[2], KATHLEEN A. CAMPBELL[1],
BRUCE A. MARSHALL[3], MIKE COLLINS[1] & ANDREA C. ALFARO[4]

[1]*Geology, School of Environment, University of Auckland, Private Bag 92019, Auckland Mail Centre, Auckland 1142, New Zealand.*
E-mail: k.saether@auckland.ac.nz; ka.campbell@auckland.ac.nz; mikecollins@slingshot.co.nz
[2]*School of Earth and Environment, University of Leeds, Leeds, LS2 9JT, United Kingdom. E-mail: c.little@see.leeds.ac.uk*
[3]*Museum of New Zealand Te Papa Tongarewa, P.O. Box 467, 169 Tory Street, Te Aro, Wellington 6011, New Zealand.*
E-mail: brucem@tepapa.govt.nz
[4]*Division of Applied Sciences, Auckland University of Technology, Private Bag 92006, Auckland 1020, New Zealand.*
E-mail andrea.alfaro@aut.ac.nz
[5]*Corresponding author*

Table of contents

Abstract

Bathymodiolus (*sensu lato*) *heretaunga* **sp. nov.** and *Gigantidas coseli* **sp. nov.** are described from Miocene-age hydrocarbon seep carbonates of North Island, New Zealand, adding to only four described fossil hydrocarbon seep mussel species. Both new species are small compared to their modern congeners, and it is suggested that an evolutionary trend toward gigantism occurred in vent and seep mussels since the first known fossil species of the group appeared in the Middle Eocene. *Bathymodiolus heretaunga* is highly variable in morphology, potentially reflecting population variation over a wide geographic area. *Gigantidas coseli* is the first named species, fossil or modern, of its genus known from hydrocarbon seeps, although several closely related species in the same group, the *Bathymodiolus childressi* clade, have been reported from these environments.

Key words: *Bathymodiolus*; cold seep; Bathymodiolinae; *Gigantidas*; new species

Accepted by R. Bieler: 17 Jul. 2010; published: 26 Aug. 2010

Introduction

All mussel species found at modern hydrocarbon seep and hydrothermal vents are currently assigned to Bathymodiolinae (see below for remarks on the current status of this taxon). They were first recorded by Lonsdale (1977) at hydrothermal vents of the Galápagos Rift, and described by Kenk and Wilson (1985) as *Bathymodiolus thermophilus* in a new subfamily Bathymodiolinae. Since this initial discovery, there have been steady additions of new bathymodioline species, such that up to 51 living species (26 species and one subspecies formally described and named, Table 1; nearly as many still undescribed, Table 2) are now assigned to the group (Kenk and Wilson 1985; Cosel *et al.* 1994; Hashimoto and Okutani 1994; Gustafson *et al.* 1998; Cosel and Olu 1998; Cosel *et al.* 1999; Hashimoto 2001; Cosel 2002; Cosel and Marshall 2003; Okutani *et al.* 2004; Smith *et al.* 2004; Hashimoto and Yamane 2005; McKiness *et al.* 2005; Jones and Vrijenhoek 2006; Cordes *et al.* 2007; Hashimoto and Furuta 2007; Olu-Le Roy *et al.* 2007; Cosel 2008a, b; Cosel and Janssen 2008; Génio *et al.* 2008; Fujita *et al.* 2009; Cosel and Marshall 2010). All species are chemosymbiotic, primarily deriving their nutrition from bacteria hosted in the gill tissues (e.g. Fujita *et al.* 2009). The most recent addition is a species found near Calyptogena Canyon, Makran accretionary prism, off Pakistan (Cosel 2008b; R. von Cosel, pers. comm. 2009). Vent and seep mussels comprise four genera: *Bathymodiolus* Kenk and Wilson, 1985, *Gigantidas* Cosel and B. Marshall, 2003, *Tamu* Gustafson, Turner, Lutz and Vrijenhoek, 1998, and *Vulcanidas* Cosel and B. Marshall, 2010. *Bathymodiolus* is by far the most speciose of these, and genetic studies (e.g. Jones *et al.* 2006) have shown it to be paraphyletic, as currently used. In consequence, at least two further genera may need to be erected for some *Bathymodiolus* species in the future, of which one (or more) should be introduced for species currently assigned to *Bathymodiolus* (*sensu lato*) (Cosel and Janssen 2008; see Table 1 and discussion of genus herein). The smallest described living vent or seep mussel is *Bathymodiolus* (*s. l.*) *taiwanensis* Cosel, 2008a, reaching a maximum shell length of 56 mm, but the majority are much larger, with shells of *Bathymodiolus boomerang* Cosel and Olu, 1998 attaining lengths of up to 360 mm.

Only species of *Bathymodiolus* and those assigned to *Bathymodiolus* (*sensu lato*) have previously been reported from fossil hydrocarbon seep assemblages, and up to five species have been at least tentatively recognized before this study, of which one, from central Japan, remains undescribed (Table 3). This latter species, from the Pliocene Tamari Formation, is known from only one specimen and its internal details are unknown and taxonomic position uncertain. It is not thought to be conspecific with the other reported Japanese fossil hydrocarbon seep mussel, *B.* (*s. l.*) *akanudaensis* (Kuroda, 1931), which is geographically and stratigraphically disjunct (Table 3) and exhibits differences in shell shape and umbonal position (T. Nobuhara, pers. comm. 2009). Species-level identification is difficult in fossil hydrocarbon seep mussels because of conservative shell morphology, and mode of their preservation in hydrocarbon seep deposits, in that the seep environment is rather corrosive, leading to rapid shell dissolution. Thus, formal descriptions of fossil material are normally limited, and taxonomic placement is usually tentative and/or has been subject to new combination(s) by later study (e.g. Moroni 1966; Kiel 2006).

Previous work on fossil mussels from the Miocene New Zealand localities of this study identified three possible morphotypes (Campbell *et al.* 2008) after initial morphometric analysis of some of the specimens reported herein (Collins 1999). Collins (1999) regarded one New Zealand morphotype as conspecific with *Bathymodiolus* (*s. l.*) *aduloides* Hashimoto and Okutani, 1994, and left the two other morphotypes in open nomenclature as ?*Bathymodiolus* species A and B. Campbell *et al.* (2008) suggested an affinity of one morphotype to *Gigantidas* and noted the superficial similarity of one of the other morphotypes to *B. aduloides*. Here, using Collins' and newly collected material, we place *B. aduloides* and ?*B.* sp A of Collins (1999) into a single, morphologically plastic species named *Bathymodiolus heretaunga*, and ?*B.* sp. B of Collins (1999) into *Gigantidas coseli*, the first formal description of a fossil species of this genus.

TABLE 1. Distribution of described modern vent and seep mussel species. Species are grouped by clade (after Samadi *et al.* 2007; Cosel and Janssen 2008; Won *et al.* 2008), with hydrothermal vent localities shaded to distinguish them from hydrocarbon seep localities.

Species	Locality, Ocean	Latitude/Longitude	Depth (m)	Reference(s)
Bathymodiolus (*s. l.*) *aduloides* clade:				
Bathymodiolus (*s. l.*) *aduloides* Hashimoto and Okutani, 1994	Iheya Ridge, NW Pacific	027°33'N / 126°58'E	1378–1389	Hashimoto and Okutani (1994); Iwasaki *et al.* (2006); Fujita *et al.* (2009)
	Minami-Ensei Knoll, NW Pacific	028°24'N / 127°38'E	679	Hashimoto and Okutani (1994)
	Off Kikaijima Island, NW Pacific	028°26'N / 130°19'E	1451	Iwasaki *et al.* (2006); Fujita *et al.* (2009)
	Okinoyama Bank, NW Pacific	034°58'N / 139°32'E	1128	Hashimoto and Okutani (1994)
Bathymodiolus (*s. l.*) *manusensis* Hashimoto and Furuta, 2007	DESMOS site, SW Pacific	003°42'S / 151°52'E	1900	Hashimoto and Furuta (2007)
	PACMANUS Field E, SW Pacific	003°44'S / 151°40'E	1627–1694	Miyazaki *et al.* (2004); Hashimoto and Furuta (2007)
Bathymodiolus (*s. l.*) *childressi* clade:				
Bathymodiolus (*s. l.*) *anteumbonatus* Cosel and Janssen, 2008	Edison Seamount, SW Pacific	003°19'S / 152°35'E	1146–1610	Krylova and Janssen (2006); Jones and Vrijenhoek (2006); Cosel and Janssen (2008)
Bathymodiolus (*s. l.*) *childressi* Gustafson, Turner, Lutz and Vrijenhoek, 1998	Alamiños Canyon, NW Gulf of Mexico	026°21'N / 094°29–30'W	540–2222	Gustafson *et al.* (1998); Jones *et al.* (2006); Olu-Le Roy *et al.* (2007)
	Green Canyon-929, NW Gulf of Mexico	027°04'N / 091°41'W	642	Carney *et al.* (2006)
	Garden Banks, NW Gulf of Mexico	027°33–37'N / 092°11–32'W	567–700	Brooks *et al.* (1989); Carney *et al.* (2006)
	Green Canyon-272, NW Gulf of Mexico	027°41'N / 091°32–33'W	527–737	Gustafson *et al.* (1998)
	Green Canyon-233, NW Gulf of Mexico	027°43'N / 091°16–18'W	559–651	Gustafson *et al.* (1998); Olu-Le Roy *et al.* (2007); Carney *et al.* (2006)
	Green Canyon-234, NW Gulf of Mexico	027°44'N / 091°13'W	527–538	Carney *et al.* (2006)
	Green Canyon-232, NW Gulf of Mexico	027°44'N / 091°19'W	---	Fujita *et al.* (2009)
	Green Canyon-237, NW Gulf of Mexico	027°46'N / 091°07'W	561	Carney *et al.* (2006)
	Bush Hill, NW Gulf of Mexico	027°47'N / 091°30–31'W	540–553	Gustafson *et al.* (1998); Kennish *et al.* (1998); Carney *et al.* (2006)
	Green Canyon-168, NW Gulf of Mexico	027°50'N / 092°10'W	650	Kennish *et al.* (1998)
Bathymodiolus (*s. l.*) *edisonensis* Cosel and Janssen, 2008	Edison Seamount, SW Pacific	003°19'S / 152°35'E	1342–1610	Cosel and Janssen (2008)
Bathymodiolus (*s. l.*) *hirtus* Okutani, Fujikura and Sasaki, 2004	Kuroshima Knoll, NW Pacific	024°08'N / 124°11–12'E	637–644	Okutani *et al.* (2004); Iwasaki *et al.* (2006); Fujita *et al.* (2009)

continued next page

TABLE 1. (continued)

Species	Locality, Ocean	Latitude/Longitude	Depth (m)	Reference(s)
Bathymodiolus (*s. l.*) *japonicus* Hashimoto and Okutani, 1994	Minami-Ensei Knoll, NW Pacific	028°23–24'N / 127°38–39'E	705–718	Hashimoto and Okutani (1994); Miyazaki *et al.* (2004); Fujita *et al.* (2009)
	Okinoyama Bank, NW Pacific	034°58'N / 139°32'E	1128	Hashimoto and Okutani (1994)
	W Sagami Bay, NW Pacific	035°00–60'N / 139°14'E	1170–1180	Hashimoto and Okutani (1994); Iwasaki *et al.* (2006)
Bathymodiolus (*s. l.*) *mauritanicus* Cosel, 2002	West Africa, E Atlantic	000°53'N / 005°28'W	1000–1267	Jones *et al.* (2006); Fujita *et al.* (2009)
	Off Banc d'Arguin, E Atlantic	018°41'N / 016°45'W	~1200[a]	Cosel (2002)
Bathymodiolus (*s. l.*) *platifrons* Hashimoto and Okutani, 1994	Dai-yon (No. 4) Yonaguni Knoll, NW Pacific	024°50'N / 122°42'E	1336	Iwasaki *et al.* (2006)
	Hatoma Knoll, NW Pacific	024°51'N / 123°50'E	1523	Iwasaki *et al.* (2006)
	Izena Cauldron, NW Pacific	027°16'N / 127°05'E	1340	Hashimoto and Okutani (1994)
	Iheya Ridge, NW Pacific	027°33–47'N / 126°54–59'E	1028–1410	Hashimoto and Okutani (1994); Miyazaki *et al.* (2004); Fujita *et al.* (2009)
	Okinoyama Bank, NW Pacific	034°58'N / 139°31'E	1180	Hashimoto and Okutani (1994)
	W Sagami Bay, NW Pacific	034°60–35°60'N / 139°14'E	1170–1180	Hashimoto and Okutani (1994); Miyazaki *et al.* (2004); Iwasaki *et al.* (2006); Fujita *et al.* (2009)
Bathymodiolus (*s. l.*) *securiformis* Okutani, Fujikura and Sasaki, 2004	Kuroshima Knoll, NW Pacific	024°08'N / 124°11–12'E[b]	637–642	Okutani *et al.* (2004); Iwasaki *et al.* (2006); Fujita *et al.* (2009)
	Dai-ni (No. 2) Atsumi Knoll, NW Pacific	033°52'N / 137°23'E	1042	Iwasaki *et al.* (2006); Fujita *et al.* (2009)
Bathymodiolus (*s. l.*) *taiwanensis* Cosel, 2008a	Off Kueishan Island, NW Pacific	024°50–51'N / 121°60'E	200–355	Cosel (2008a)
Bathymodiolus (*s. l.*) *tangaroa tangaroa* Cosel and B. Marshall, 2003	Off Cape Turnagain, SW Pacific	040°26'S / 176°58'E[c]	920–1205	Cosel and Marshall (2003); Smith *et al.* (2004); Jones *et al.* (2006); Fujita *et al.* (2009)
Bathymodiolus (*s. l.*) *tangaroa tuerkayi* Cosel and Janssen, 2008	Edison Seamount, SW Pacific	003°19'S / 152°35'E	1448–1610	Cosel and Janssen (2008)
Gigantidas gladius Cosel and B. Marshall, 2003	Rumble V submarine volcano, SW Pacific	036°08'S / 178°12'E	360–755	Cosel and Marshall (2003)
	Rumble III submarine volcano, SW Pacific	035°44–45'S / 178°29–30'E	216–460	Cosel and Marshall (2003); Jones and Vrijenhoek (2006); Fujita *et al.* (2009)
	Macauley Cone	030°13'S / 178°27'E	200	Fujita *et al.* (2009)
Gigantidas horikoshii Hashimoto and Yamane, 2007	Kaikata Seamount, NW Pacific	026°42–43'N / 141°04–05'E	435–762	Hashimoto and Yamane (2005); Fujita *et al.* (2009)

continued next page

TABLE 1. (continued)

Species	Locality, Ocean	Latitude/Longitude	Depth (m)	Reference(s)
Bathymodiolus (*s. s.*) *thermophilus* clade:				
Bathymodiolus (*s. s.*) *azoricus* Cosel and Comtet in Cosel, Comtet and Krylova, 1999	Lucky Strike hydrothermal field, E Atlantic	037°17–18'N / 032°15–17'W	866–2330	Cosel *et al.* (1999); Jones *et al.* (2006); Fujita *et al.* (2009)
	Menez Gwen hydrothermal field, E Atlantic	037°51'N / 031°31'W	824–877	Cosel *et al.* (1999); Olu-Le Roy *et al.* (2007)
Bathymodiolus (*s. s.*) *boomerang* Cosel and Olu, 1998	Barbados accretionary prism, W Atlantic	010°20'N / 058°37–53'W	697–950^{d}	Cosel and Olu (1998)
Bathymodiolus (*s. s.*) *brevior* Cosel, Métivier and Hashimoto, 1994	Vailili vent field, SW Pacific	023°13'S / 176°37–38'W	1703–1757	Cosel *et al.* (1994); Fujita *et al.* (2009)
	Hine Hina hydrothermal field, SW Pacific	022°32'S / 176°43'W	1842–1853	Cosel *et al.* (1994)
	Mussel Valley, SW Pacific	018°50'S / 173°29'W	2750	Cosel *et al.* (1994)
	White Lady hydrothermal field, SW Pacific	016°59–60'S / 173°45–55'W	1990–2750	Cosel *et al.* (1994); Olu-Le Roy *et al.* (2007)
Bathymodiolus (*s. s.*) *brooksi* Gustafson, Turner, Lutz and Vrijenhoek, 1998	West Florida Escarpment, NE Gulf of Mexico	026°02–03'N / 084°54–55'W	3270–3314	Gustafson *et al.* (1998); Kennish *et al.* (1998); Fujita *et al.* (2009)
	Alamiños Canyon, NW Gulf of Mexico	026°21'N / 094°29–30'W	2220–2340	Gustafson *et al.* (1998); Kennish *et al.* (1998); Jones *et al.* (2006); Olu-Le Roy *et al.* (2007)
	Atwater Valley, N Gulf of Mexico	027°34'N / 088°30'W	1893	Cordes *et al.* (2007)
Bathymodiolus (*s. s.*) *elongatus* Cosel, Métivier and Hashimoto, 1994	North Fiji Basin, SW Pacific	018°50'S / 173°29' W	2720–2765	Cosel *et al.* (1994); Olu-Le Roy *et al.* (2007)
Bathymodiolus (*s. s.*) *heckerae* Turner, Gustafson, Lutz and Vrijenhoek in Gustafson *et al*., 1998	West Florida Escarpment, NE Gulf of Mexico	026°01–03'N / 084°54–56'W	3243–3314	Gustafson *et al.* (1998); Kennish *et al.* (1998); Jones *et al.* (2006); Olu-Le Roy *et al.* (2007)
	Blake Ridge, E Atlantic	032°30'N / 076°11'W	2155	Van Dover *et al.* (2003); Jones *et al.* (2006)
Bathymodiolus (*s. s.*) *marisindicus* Hashimoto, 2001	Kairei Field, C Indian Ocean	025°19'S / 070°02'E	2415–2460	Hashimoto (2001); Van Dover *et al.* (2001); McKiness and Cavanaugh (2005); Iwasaki *et al.* (2006); Fujita *et al.* (2009)
	Edmond Field, C Indian Ocean	023°52–53'S / 069°35–36'E	3289–3320	McKiness and Cavanaugh (2005); Jones *et al.* (2006); Fujita *et al.* (2009)
Bathymodiolus (*s. s.*) *puteoserpentis* Cosel, Comtet and Krylova, 1999	Logatchev hydrothermal field, C Atlantic	014°45'N / 044°59'W	3065	Olu-Le Roy *et al.* (2007)
	Snake Pit hydrothermal field, C Atlantic	023°22'N / 044°56–047°57'W	3023–3521	Kennish *et al.* (1998); Cosel *et al.* (1999); Jones *et al.* (2006); Fujita *et al.* (2009)
Bathymodiolus (*s. s.*) *septemdierum* Hashimoto and Okutani, 1994	Mariana Back-Arc Basin, W Pacific	018°13'N / 144°42'E	3600	Iwasaki *et al.* (2006)
	Hatoma Knoll, NW Pacific	024°51'N / 123°50'E	1523	Iwasaki *et al.* (2006); Fujita *et al.* (2009)
	Mokuyo Seamount, NW Pacific	028°19'N / 140°39'E	1256	Hashimoto and Okutani (1994)
	Suiyo Seamount, NW Pacific	028°34'N / 140°39'E	1367–1382	Hashimoto and Okutani (1994); Miyazaki *et al.* (2004); Iwasaki *et al.* (2006); Fujita *et al.* (2009)
	Myojin Knoll, NW Pacific	032°06'N / 139°52'E	1288–1346	Miyazaki *et al.* (2004); Fujita *et al.* (2009)

continued next page

TABLE 1. (continued)

Species	Locality, Ocean	Latitude/Longitude	Depth (m)	Reference(s)
Bathymodiolus (*s. s.*) *thermophilus* Kenk and Wilson, 1985	East Pacific Rise, E Pacific	018°35'S / 113°55'W	2673	Olu-Le Roy *et al.* (2007)
		017°25'S / 113°12'W	2578–2581	Won *et al.* (2003)
		011°18'S / 110°32'W	2669	Won *et al.* (2003)
		007°26'S / 104°47'W	2460–2747	Jones *et al.* (2006)
		007°25'S / 107°48–49'W	2746–2747	Won *et al.* (2003); Fujita *et al.* (2009)
		009°33–34'N / 104°14–15'W	2567	Gustafson *et al.* (1998); Won *et al.* (2003)
		009°41'N / 104°16'W	2556	Gustafson *et al.* (1998)
		009°48–51'N / 104°17–18'W	2460–2747	Gustafson *et al.* (1998); Won *et al.* (2003); Jones *et al.* (2006); Olu-Le Roy *et al.* (2007); Fujita *et al.* (2009)
		011°25'N / 103°47'W	2515	Gustafson *et al.* (1998); Won *et al.* (2003); Fujita *et al.* (2009)
		012°49'N / 103°57'W	2630–2636	Gustafson *et al.* (1998); Won *et al.* (2003)
			2228–2229	Fujita *et al.* (2009)
Not assigned:				
Tamu fisheri Gustafson, Turner, Lutz and Vrijenhoek, 1998	Bush Hill, NW Gulf of Mexico	027°47'N / 091°30'W	548	Gustafson *et al.* (1998)
	Louisiana Slope, NW Gulf of Mexico	027°50'N / 091°10'W	650–701	Gustafson *et al.* (1998)
	Garden Banks, NW Gulf of Mexico	027°50'N / 092°10'W	546–650	Jones and Vrijenhoek (2006); Fujita *et al.* (2009)
Vulcanidas insolatus Cosel and B. Marshall, 2010	Giggenbach volcano and Macauley Caldera, SW Pacific	030°02–13'S / 178°27–43'W	140–504	Smith *et al.* (2004); Jones *et al.* (2006); Cosel and Marshall (2010)

[a] Also possibly collected from a depth of approximately 400 m.

[b] Reported from 024°88'N / 124°12'E by Iwasaki *et al.* (2006); Fujita *et al.* (2009), herein regarded as typographical errors.

[c] Reported from 040°26'S / 178°58'E by Jones *et al.* (2006), herein regarded as a typographical error.

[d] Also reported from a depth of 1950 m at the same coordinates by Olu-Le Roy *et al.* (2007), herein regarded as a typographical error.

Material and methods

Fossil mussel specimens were collected during a number of field trips to 11 localities in the Hawke's Bay area (Fig. 1) over several years (1997–2009), adding to material obtained from the bulk palaeontology collection at GNS. Specimens described and figured herein are deposited in the palaeontology collection of the Geology programme, School of Environment, UOA. Modern comparative material is housed at NMNZ and NIWA.

Specimens were prepared using various methods to remove excess hydrocarbon seep-carbonate material from the shells, including a Consolidated Pneumatic Tool Co. air scribe, Burgess Professional engraver kit, dental picks, toothbrush, and water, the former three methods usually in conjunction with a light microscope, magnifying visor or hand lens. Sometimes shell material was deliberately removed from specimens to reveal internal shell features. Specimens were photographed using a Nikon D300 Digital SLR camera with an AF-S Micro Nikkor 60 mm f/2.8 G ED lens. Specimens were whitened with ammonium chloride before photography, and some images were edited in Adobe Photoshop CS4 to enhance contrast and some shell details. Subtle shell features were drawn onto comparative figures using Adobe Illustrator CS4, which also was the software used to place individual images into compound figures. Measurements were taken with vernier callipers to within an error of 0.1 mm for a total of 248 individuals.

Abbreviations used in the text

A	anterior length (distance from beaks to anterior margin)
AU	(preceding five-digit number) collection number, UOA
BX	Bexhaven site
f	(succeeding map sheet number and preceding four-digit number) fossil locality number, registered in archival New Zealand Fossil Record File maintained jointly by GNS and GSNZ
GNS	GNS Science, 1 Fairway Drive, Avalon, Lower Hutt 5010, P.O. Box 30368, Lower Hutt 5040, New Zealand
GSNZ	Geological Society of New Zealand, P.O. Box 38591, Wellington Mail Centre, Lower Hutt 5045, New Zealand
GS	(preceding four- or five-digit number) fossil locality number, GNS
H	shell height
I	shell inflation (both valves)
KK	Karikarihuata site
L	shell length
L	(preceding four-digit number) bivalve specimen number, palaeontology collection, UOA
MN	Moonlight North site
n	number of specimens
NIWA	National Institute for Water and Atmospheric Research, 301 Evans Bay Parade, Hataitai, Wellington 6021, Private Bag 14901, New Zealand
NMNZ	Museum of New Zealand Te Papa Tongarewa, 169 Tory Street, Te Aro, P.O. Box 467, Wellington 6011, New Zealand
PK	Puketawa site
RK	Rocky Knob site
SD	standard deviation
s. l.	sensu lato
s. s.	sensu stricto
TM	(preceding four-digit number) type molluscan specimen number, palaeontology collection, GNS
TT	Totaranui site
TW	Tauwhareparae site
U	umbonal position as percentage along shell length from anterior margin
UOA	Geology, School of Environment, University of Auckland, Private Bag 92019, Auckland Mail Centre, Auckland 1142, New Zealand

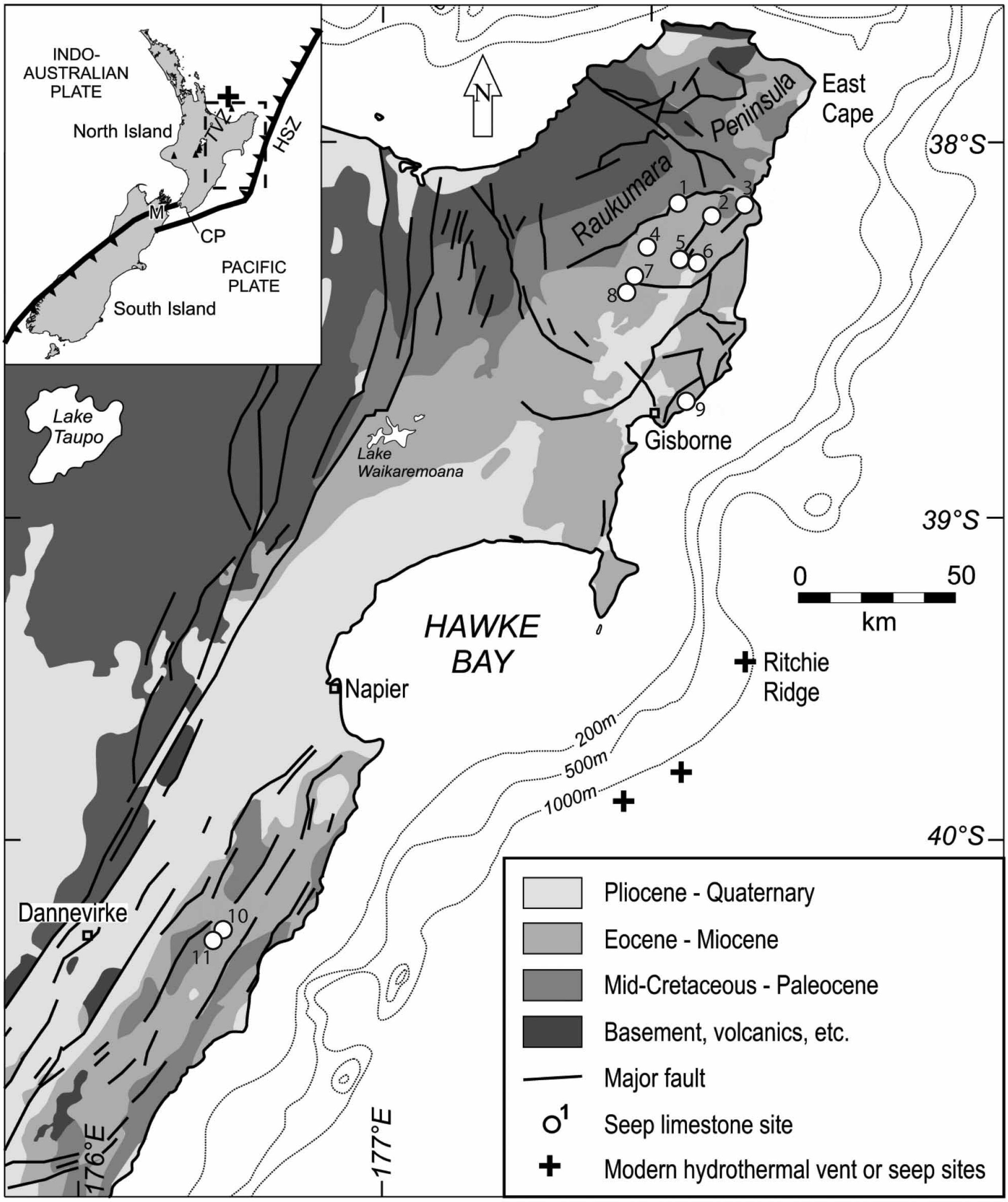

FIGURE 1. Overview of relevant geology of the East Coast Basin, North Island, New Zealand, showing locations of the Miocene fossil hydrocarbon seep carbonates from which specimens of *Bathymodiolus heretaunga* **sp. nov.** and *Gigantidas coseli* **sp. nov.** were collected. 1–9. Sites of the northern region. 1. Bexhaven. 2. Karikarihuata. 3. Waipiro. 4. Tauwhareparae. 5. Puketawa. 6. Totaranui. 7. Moonlight North. 8. Rocky Knob. 9. Turihaua. 10, 11. Sites of the southern region. 10. Wanstead. 11. Ugly Hill. CP: Cape Palliser; HSZ: Hikurangi Subduction Zone; M: Marlborough; TVZ: Taupo Volcanic Zone. Also shown are some of the modern offshore hydrocarbon seep and hydrothermal vent sites on the Hikurangi Margin. Inset shows the Hikurangi subduction zone as part of the transpressive boundary between the Indo-Australian and Pacific Plates. Figure modified from Campbell *et al.* (2008).

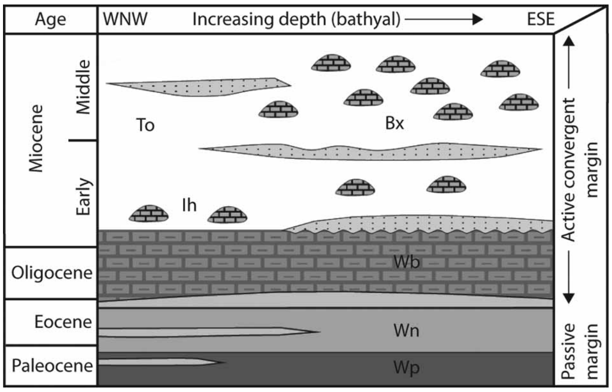

FIGURE 2. Generalized stratigraphy of the East Coast Basin, showing schematically the Miocene-age hydrocarbon seep carbonates that occur as isolated lenses with in the mudstones of the Tolaga Group. The organic-rich, underlying Waipawa Black Shale is thought to be one of the likely source rocks. Bx: Bexhaven Limestone; ESE: east-south-east; Ih: Ihungia Limestone; To: Tolaga Group; Wb: Weber Formation; Wn: Wanstead Formation; WNW: west-north-west; Wp: Waipawa Black Shale. Figure modified from Campbell *et al.* (2008).

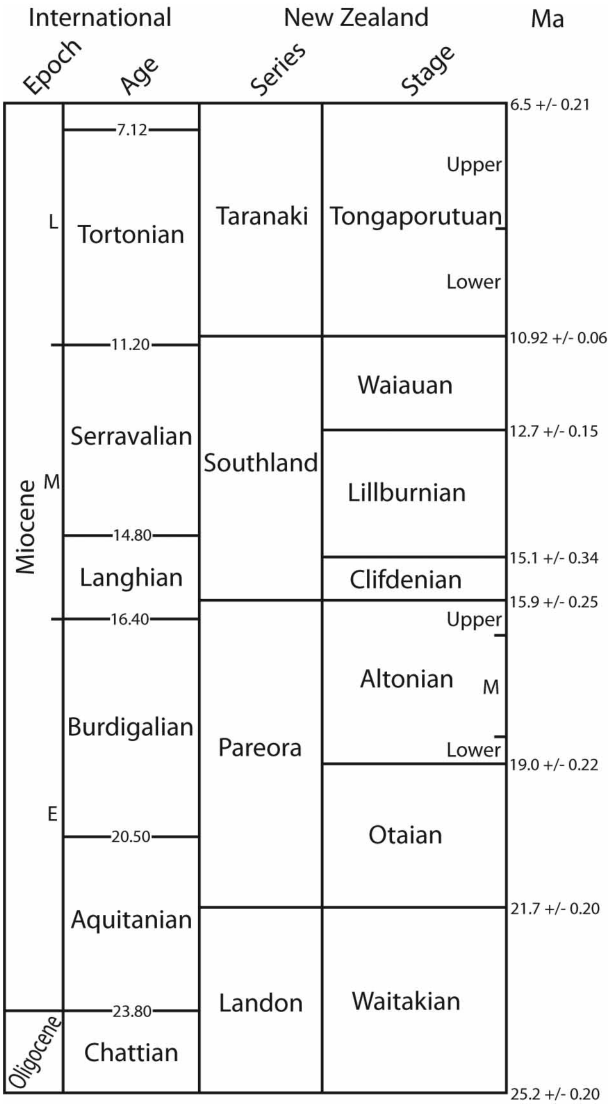

FIGURE 3. Geological timescale to show correlation of Miocene New Zealand series and stages with the international standard epochs and ages. E: Early; L: Late; M: Middle; Ma: million years. Modified from Cooper (2004).

TABLE 2. Distribution of modern vent and seep mussel species still in open nomenclature, with hydrothermal vent localities shaded to distinguish them from hydrocarbon seep localities.

Species Designation	Locality, Ocean	Latitude/Longitude	Depth (m)	Reference(s)
Bathymodiolus cf. *thermophilus* Jones and Vrijenhoek, 2006	32°S East Pacific Rise, SE Pacific	031°52'S / 112°03'W	2331	Won *et al.* (2003); Jones *et al.* (2006); Fujita *et al.* (2009)
	31°S East Pacific Rise, SE Pacific	031°09'S / 111°56'W	2332–2333	Won *et al.* (2003); Fujita *et al.* (2009)
Bathymodiolus (*s. l.*) sp. Cosel, unpublished	Calyptogena Canyon, N Indian[1]	064°15'N / 024°25'E	2220	Cosel (pers. comm. 2009)
Bathymodiolus sp. A Olu-Le Roy, Cosel, Hourdez, Carney and Jollivet, 2007	Nigerian Slope, E Atlantic	004°59'S / 004°08'E	1000–1700	Cordes *et al.* (2007)
	REGAB site, E Atlantic	005°48'S / 009°43'E	3151–3170	Olu-Le Roy *et al.* (2007)
Bathymodiolus sp. aff. *puteoserpentis* Cosel, Comtet and Krylova, 1999	Logatchev hydrothermal field, C Atlantic	014°45'S / 044°58'E	2930	Cosel *et al.* (1999)
	Irina site, C Atlantic	014°45'S / 044°49'E	3040–3063	Cosel *et al.* (1999)
Bathymodiolus sp. B Cordes, Carney, Hourdez, Carney, Brooks and Fisher, 2007	Nigerian Slope, E Atlantic	004°59'S / 004°08'E	1000–1700	Cordes *et al.* (2007)
Bathymodiolus sp. B Olu-Le Roy, Cosel, Hourdez, Carney and Jollivet, 2007[2]	Orénoque A, W Atlantic	010°19–20'N / 058°53–54'W	1688–1690	Cosel (2002); Olu-Le Roy *et al.* (2007); Génio *et al.* (2008)
	El Pilar, W Atlantic	011°14'N / 059°22'W	1200	Olu-Le Roy *et al.* (2007)
Bathymodiolus sp. Chamorro Fujita, Matsumoto, Fujiwara, Hashimoto, Galkin, Ueshima and Miyazaki, 2009	Chamorro Seamount, NW Pacific	013°47'N / 146°00'E	2899	Fujita *et al.* (2009)
Bathymodiolus sp. Eifuku Fujita, Matsumoto, Fujiwara, Hashimoto, Galkin, Ueshima and Miyazaki, 2009	Eifuku Seamount, NW Pacific	021°29'N / 144°02'E	1625	Fujita *et al.* (2009)
Bathymodiolus (*s. l.*) sp. GOC Génio, Johnson, Vrijenhoek, Cunha, Tyler, Kiel and Little, 2008[2]	Gulf of Cadiz, E Atlantic	035°24'N / 007°11'W	1115	Génio *et al.* (2009)
Bathymodiolus sp. IV Cosel, unpublished	Mound 12, E Pacific[3]	008°56'N / 084°19'W	960–1015	Bohrmann *et al.* (2002); Han *et al.* (2004)
Bathymodiolus sp. JdF McKiness, McMullin, Fisher and Cavanaugh, 2005	Endeavour Vent Field, NE Pacific	047°56'N / 129°06'W	~2200	McKiness *et al.* (2005)
Bathymodiolus sp. Kikaijima Fujita, Matsumoto, Fujiwara, Hashimoto, Galkin, Ueshima and Miyazaki, 2009	Off Kikaijima Island, NW Pacific	028°26'N / 130°19'E	1430	Fujita *et al.* (2009)
Bathymodiolus sp. Lau 1 Fujita, Matsumoto, Fujiwara, Hashimoto, Galkin, Ueshima and Miyazaki, 2009[4]	Lau Basin, SW Pacific	023°32'S / 176°43'E	1818	Fujita *et al.* (2009)
Bathymodiolus sp. Lau 2 Fujita, Matsumoto, Fujiwara, Hashimoto, Galkin, Ueshima and Miyazaki, 2009[4]	Lau Basin, SW Pacific	023°32'S / 176°43'E	1818	Fujita *et al.* (2009)

continued next page

TABLE 2. (continued)

Species Designation	Locality, Ocean	Latitude/Longitude	Depth (m)	Reference(s)
Bathymodiolus sp. Kikaijima Fujita, Matsumoto, Fujiwara, Hashimoto, Galkin, Ueshima and Miyazaki, 2009	Off Kikaijima Island, NW Pacific	028°26'N / 130°19'E	1430	Fujita *et al.* (2009)
Bathymodiolus sp. NZ Fujita, Matsumoto, Fujiwara, Hashimoto, Galkin, Ueshima and Miyazaki, 2009[4]	Off New Zealand	---	---	Fujita *et al.* (2009)
Bathymodiolus sp. Sissano 1 Fujita, Matsumoto, Fujiwara, Hashimoto, Galkin, Ueshima and Miyazaki, 2009	Sissano, SW Pacific	002°49'N / 142°14'E 002°53'N / 142°16'E	1881 1646	Fujita *et al.* (2009) Fujita *et al.* (2009)
Bathymodiolus sp. Sissano 2 Fujita, Matsumoto, Fujiwara, Hashimoto, Galkin, Ueshima and Miyazaki, 2009	Sissano, SW Pacific	002°49'N / 142°14'E	1881	Fujita *et al.* (2009)
Bathymodiolus sp. Sissano 3 Fujita, Matsumoto, Fujiwara, Hashimoto, Galkin, Ueshima and Miyazaki, 2009	Sissano, SW Pacific	002°49'N / 142°14'E	1881	Fujita *et al.* (2009)
Bathymodiolus sp. V Cosel, 2002	Mariana Back-Arc Basin, NW Pacific	018°13'N / 144°42–43'E	3589–3600	Cosel (2002); Jones *et al.* (2006); Iwasaki *et al.* (2006); Fujita *et al.* (2009)
Gigantidas sp. Baco, Rowden, Levin, Smith and Bowden, 2010[5]	Builder's Pencil, SW Pacific	039°54'S / 178°33'E	800	Baco *et al.* (2010)
Gigantidas sp. Aitape Fujita, Matsumoto, Fujiwara, Hashimoto, Galkin, Ueshima and Miyazaki, 2009	Aitape, SW Pacific	002°55'S / 142°14'E	470	Fujita *et al.* (2009)
Gigantidas sp. Ashizuri Fujita, Matsumoto, Fujiwara, Hashimoto, Galkin, Ueshima and Miyazaki, 2009	Off Ashizuri Cape, NW Pacific	032°39'N / 133°37'E	575	Fujita *et al.* (2009)
Gigantidas sp. Nikko Fujita, Matsumoto, Fujiwara, Hashimoto, Galkin, Ueshima and Miyazaki, 2009[6]	Nikko Seamount, NW Pacific	023°05'N / 142°19'E	485	Fujita *et al.* (2009)
Gigantidas sp. Sumisu Fujita, Matsumoto, Fujiwara, Hashimoto, Galkin, Ueshima and Miyazaki, 2009[6]	Sumisu Caldera, NW Pacific	031°28'N / 140°04'E	676–686	Fujita *et al.* (2009)

---

[1] Locality data retrieved from Rad *et al.* (2002).

[2] Possibly synonymous with *Bathymodiolus mauritanicus* Cosel, 2002, *B.* sp. B of Olu-Le Roy *et al.* (2007) being somewhat larger than the described population, *B.* sp. GOC of Génio *et al.* (2008) being somewhat smaller.

[3] Locality data retrieved from Mau *et al.* (2006).

[4] Probably synonymous with *Bathymodiolus manusensis* Hashimoto and Furuta, 2007 (Fujita *et al.* 2009).

[5] Possibly synonymous with *Gigantidas gladius* Cosel and B. Marshall, 2003 (Marshall, unpublished; R. von Cosel, pers. comm. 2009).

[6] Probably synonymous with *Gigantidas horikoshii* Hashimoto and Yamane, 2005 (Fujita *et al.* 2009).

TABLE 3. Summary of age and occurrence of fossil vent and seep mussel species from hydrocarbon seep deposits recognized before this study.

Species	Age	Occurrence	Reference(s)
Bathymodiolus? sp.; Nobuhara, 2003	Pliocene	Tamari Formation, central Japan	Nobuhara (2003)
Bathymodiolus? *exbrocchii* (Sacco, 1898)	Upper Miocene	Calcari a *Lucina*, NE Italy	Moroni (1966); Taviani (1994)
Bathymodiolus (*s. l.*) *akanudaensis* (Kuroda, 1931)	Upper Miocene	Ogaya Formation, central Japan	Amano and Kanno (2005); Amano *et al.* (2010)
	Middle Miocene	Middle Bessho Formation, central Japan	Tanaka (1959); Majima *et al.* (2005); Nobuhara *et al.* (2008); Amano *et al.* (2010)
Bathymodiolus (*s. l.*) *palmarensis* Kiel, Campbell and Gaillard, 2010	Lower Miocene	Pozon Formation, Venezuela	Kiel *et al.* (2010); Gill (2005); Gill *et al.* (2005)
	?Oligocene	Palmar-Molinera-Road site, N Colombia	Kiel *et al.* (2010)
Bathymodiolus willapaensis (Squires and Goedert, 1991)	Upper Oligocene	Pysht Formation, NW USA	Goedert and Squires (1993); Goedert *et al.* (2003)
	Lower Oligocene	Makah Formation, NW USA	Goedert and Campbell (1995); Squires and Goedert (1995)
		Lincoln Creek Formation, NW USA	Campbell and Bottjer (1993); Goedert and Squires (1993)
	Upper Eocene	Bear River Deposit, NW USA	Squires and Goedert (1991); Campbell and Bottjer (1993)
		Lincoln Creek Formation, NW USA	Campbell and Bottjer (1993)
	Middle–Upper Eocene	Humptulips Formation, NW USA	Squires and Goedert (1991, 1995); Goedert and Kaler (1996)

Geological setting

At least 16 geographically isolated fossil hydrocarbon seep deposits are present along 300 km of the uplifted East Coast Basin forearc, eastern North Island (Campbell *et al.* 2008; Fig. 1 herein). They occur in two distinct regions, the Raukumara Peninsula and near Dannevirke, which are situated to the north and south of the Hawke's Bay region, respectively, where they occur as discrete pods or lenses of authigenic carbonate enclosed within thick siliciclastic mudstone deposits (Fig. 2).

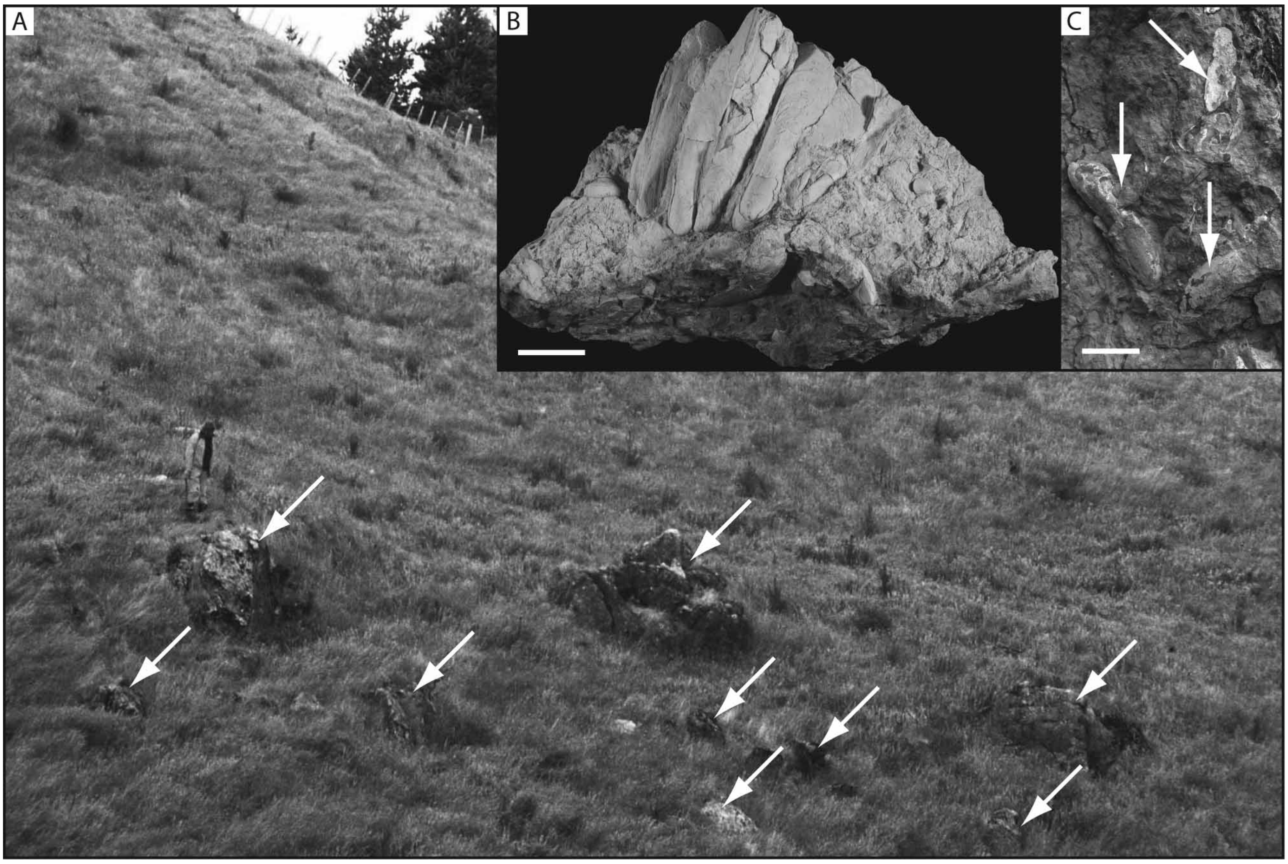

FIGURE 4. Images showing typical hydrocarbon seep carbonate deposit and appearance of New Zealand hydrocarbon seep mussels in field samples before curating. A. Several float boulders (arrowed) originating upslope at Moonlight North locality. Person for scale. B. Clustered specimens of *Gigantidas coseli* **sp. nov.** occurring in situ from Bexhaven locality. Scale bar is 20 mm. C. Ex situ occurrence of specimens of *G. coseli* (arrowed) from Moonlight North. Scale bar is 30 mm.

The East Coast Basin formed as a result of subduction of the north-westward moving Pacific Plate beneath the overriding Australian Plate, which has been ongoing since the Early Miocene (Ballance 1976; Ansell and Bannister 1996). Extending roughly 650 km north to south, the East Coast Basin varies in width from 60 to 110 km, bounded to the west by NNE–SSW trending axial mountain ranges and extending offshore to its eastern boundary along the similarly trending modern Hikurangi Trough (Fig. 1). The western onshore deposits represent an exhumed forearc, its sediments having been generated during a period of oblique convergence along the Hikurangi subduction zone since the Early Miocene (Ballance 1976; Barnes *et al.* 2002). They accumulated during onset of intense deformation, the appearance of andesitic volcanism to the west, and abrupt changes in sedimentation rate and character (Rait *et al.* 1991). Today, the Hikurangi margin constitutes the southern extremity of the Tonga–Kermadec–Hikurangi–Macquarie seismic zone, a west-facing subduction system oriented roughly parallel to the East Coast of North Island.

Bathymodiolus (*s. l.*) *heretaunga* occurs at 11 of the East Coast Basin hydrocarbon seeps, in both northern and southern regions: Bexhaven (NZ Lillburnian stage, Fig. 3), Karikarihuata (Lillburnian), Moonlight North (Waiauan, Fig. 4A), Puketawa (?Clifdenian–Lillburnian), Rocky Knob (Lillburnian), Tauwhareparae

(Lillburnian), Totaranui (?Lillburnian), Turihaua (Tongaporutuan), Ugly Hill (?Waitakian–Altonian), Waipiro (Otaian–Altonian), and Wanstead (Waitakian–Otaian) localities. *Gigantidas coseli* has a more restricted geographical range and occurs at five of the northern sites: Bexhaven, Moonlight North, Rocky Knob, Tauwhareparae and Turihaua. The ages of these deposits are approximate due to a lack of tight palaeontological control. There also are stratigraphic correlation limitations of the limestones within the monotonous, voluminous mudstone sequence, which is structurally complex, with major, long-active, low-angle normal faults predominating in some areas, especially in the north (Campbell *et al.* 2008).

Systematics

Class Bivalvia Linnaeus, 1758 (Buonanni, 1681)

Order Mytiloida Férussac, 1822

Family Mytilidae Rafinesque, 1815

Subfamily Bathymodiolinae Kenk and Wilson, 1985

Discussion. Vent and seep mussels of the genera *Bathymodiolus*, *Gigantidas* and *Tamu* traditionally have been referred to a subfamily Bathymodiolinae Kenk and Wilson, 1985 (e.g. Cosel and Janssen 2008), although as indicated by Samadi *et al.* (2007), on molecular evidence the group is “robustly rooted within a monophyletic group that includes the species *Modiolus modiolus*...”, i.e. subfamily Modiolinae Keen, 1958. Thus, Bathymodiolinae would appear to be a grade of Modiolinae comprising several clades, each probably independently derived from small wood-associated ancestors (Distel 2000; Fujita *et al.* 2009). Re-evaluation of the higher classification of mytilids is not our intention, and we consider it appropriate and convenient to refer to these mussels as bathymodiolines.

Genus *Bathymodiolus* Kenk and Wilson, 1985

Bathymodiolus Kenk and Wilson, 1985: 255. Type species (by original designation): *Bathymodiolus thermophilus* Kenk and Wilson, 1985.

Discussion. The genus *Bathymodiolus* currently contains 22 described species, with one subspecies. As species were steadily added to the genus since its inception, and following the tentative placement of *Bathymodiolus* (*s. l.*) *childressi* by Gustafson *et al.* (1998), Cosel (2002) instigated an overhaul of the taxonomic status of the genus, dividing it into several groups based upon a number of shell and anatomical features. These features included the form of the posterior retractor, umbonal placement, and placement of the anterior retractor scar relative to the umbonal cavity. This study has since been bolstered by molecular analyses of the genus (Miyazaki *et al*. 2004; Jones and Vrijenhoek 2006; Jones *et al.* 2006; Iwasaki *et al.* 2006; Samadi *et al.* 2007; Génio *et al.* 2008; Won *et al.* 2008; Fujita *et al.* 2009), confirming its paraphyletic status. Three clades are currently recognized within the genus *Bathymodiolus*, two within *Bathymodiolus* (*s. l.*) (the *B. aduloides* and *B. childressi* clades), and the *B. thermophilus* clade, or *Bathymodiolus* (*s. s.*) (Cosel and Janssen 2008). The clades are themselves split into smaller groups based upon differences among the above-mentioned features plus consideration of shell size, shape, and form of the anterior margin (Cosel and Janssen 2008). Several species currently referred to *Bathymodiolus* (*s. l.*) will probably eventually be referred to new genera (see also discussion of the genus *Gigantidas* below).

Bathymodiolus (*s. l.*) *heretaunga* Saether, Little, Campbell, Marshall, Collins and Alfaro sp. nov.

(Figs. 5, 6, 7, 10, 16)

?Mytilid closely resembling *Idasola* Beu & Maxwell, 1990.

Bathymodiolus aduloides.—Collins, 1999: 33, pls. 1–4, Table 1 not Hashimoto & Okutani, 1994.

?*Bathymodiolus* n. sp. A Collins, 1999.

Group 1 (G1) Collins, 1999.

Group 2 (G2) Collins, 1999.

Modiolus areolatus.—Collins, 1999: Table 1 not Gould, 1850.

Xenostrobus cf. *altijugatus* Collins, 1999 not Marwick, 1931.

Modiolus areolatus.—Campbell *et al.* 2008: 92, Table 1 not Gould, 1850.

Xenostrobus cf. *altijugatus* Campbell *et al.* 2008 not Marwick, 1931.

Smaller, stouter, flared variety that resembles ... *Bathymodiolus aduloides* Campbell *et al.*, 2008.

Holotype. Specimen TM8719, (Figs. 5A.6, B.1–4), adult, UOA, borrowed from GNS.

Type locality. Puketawa (Y16/f0580), Hawke's Bay, North Island, New Zealand; ?late Early Miocene–Middle Miocene (Clifdenian–Lillburnian) hydrocarbon seep carbonate.

Paratypes. 17 moderately to well preserved small to large specimens. Two medium sized, L4171, L4178, from Karikarihuata (Y16/f1049, Y16/f1043); one medium sized, TM8717, one large, TM8724 (Fig. 5A.8), from Puketawa (Y16/f0580); three small, L4099 (Fig. 5A.1), L4100 (Fig. 5A.2), L4201 (Fig. 5A.3), four medium sized, L4071, L4084, L4166 (Fig. 5A.5), L4198, one large, TM8727, from Rocky Knob (Y16/f0641, Y16/f1036, Y16/f1038, Y16/f1039, Y16/f1040, Y16/f1041, Y16/f1043); one small, TM8733, one large, TM8734 (Fig. 5A.7), from Tauwhareparae (Y16/f0539); one small, L4066, two medium sized, L4068, L4088, from Totaranui (Y16/f1056). All specimens at UOA, five borrowed from GNS. See Table 4 for dimensions.

TABLE 4. Selected measurements of specimens of *Bathymodiolus heretaunga* **sp. nov.** Italicized values are approximate.

Specimen	Type	A	H	I	L	H/L	L/H	U	Site
TM8719	Holotype	3.0	22.4	18.3	46.1	0.49	2.06	7%	PK
L4171	Paratype	3.8	16.7	13.0	33.9	0.49	2.03	11%	KK
L4178	Paratype	3.8	19.1	14.7	38.8	0.49	2.03	10%	KK
TM8717	Paratype	2.8	16.1	13.4	33.1	0.49	2.06	8%	PK
TM8724	Paratype	4.8	35.6	27.9	95.4	0.37	2.68	5%	PK
L4099	Paratype	0.8	5.1	3.5	8.3	0.61	1.63	10%	RK
L4100	Paratype	0.5	7.0	5.0	11.1	0.63	1.59	5%	RK
L4201	Paratype	1.9	7.7	5.4	14.7	0.52	1.91	13%	RK
L4084	Paratype	3.3	8.9	*11.4*	27.6	0.32	3.10	12%	RK
L4166	Paratype	1.8	14.8	*12.2*	30.5	0.49	2.06	6%	RK
L4198	Paratype	3.1	13.5	11.1	21.8	0.62	1.61	14%	RK
TM8728	Paratype	4.7	*20.7*	18.3	43.1	*0.48*	*2.08*	11%	RK
L4071	Paratype	4.6	11.8	12.1	32.0	0.37	2.71	14%	RK
L4066	Paratype	2.0	9.8	7.9	17.9	0.55	1.83	11%	TT
L4068	Paratype	4.5	21.9	15.6	39.7	0.55	1.81	11%	TT
L4088	Paratype	5.4	30.9	17.5	58.1	0.53	1.88	*9%*	TT
TM8733	Paratype	3.2	12.7	9.1	23.2	0.55	1.83	14%	TW
TM8734	Paratype	*4.4*	30.7	20.4	68.7	0.45	2.24	*6%*	TW

Other material. 199 poorly to well preserved small to large specimens: 19 from Bexhaven (Y16/f0566, Y16/f1032, Y16/f1048); nine from Karikarihuata (Y16/f0575, Y16/f1046, Y16/f1049, Y16/f1051, Y16/f1052, Y16/f1053); two from Moonlight North (Y16/f1033, Y16/f1054); 10 from Puketawa (Y16/f0580); 88 from Rocky Knob (Y16/f0641, Y16/f0642, Y16/f1028, Y16/f1029, Y16/f1030, Y16/f1034, Y16/f1036, Y16/f1037, Y16/f1038, Y16/f1039, Y16/f1040, Y16/f1041, Y16/f1042, Y16/f1043, Y16/f1044); nine from

Tauwhareparae (Y16/f0539, Y16/f1055); 40 from Totaranui (Y16/f0575, Y16/f1056); 16 from Ugly Hill (U23/f0266); four from Wanstead (U23/f7464); two from Waipiro (Z16/f0075, Z16/f7491). See Appendix I for dimensions and specimen data. Approximately 97 others from all localities, too poorly preserved for verifiable identification and use in descriptions. All specimens at UOA, 53 borrowed from GNS.

FIGURE 5. Growth series and holotype of *Bathymodiolus heretaunga* **sp. nov.** A. Diagnostic lateral views of left and right valves to show growth series. Scale bar is 25 mm. A.1. Paratype L4099. A.2. Paratype L4100. A.3. Paratype L4201. A.4. Specimen L4515. A.5. Paratype L4166. A.6. Holotype TM8719. A.7. Paratype TM8734. A.8. Paratype TM8724. B. Diagnostic views of holotype TM8719. B.1. Anterior view. Scale bar is 5 mm. B.2. Dorsal view. Scale bar is 10 mm. B.3. Lateral view of right valve. Scale bar is 10 mm. B.4. Lateral view of left valve. Scale bar is 10 mm.

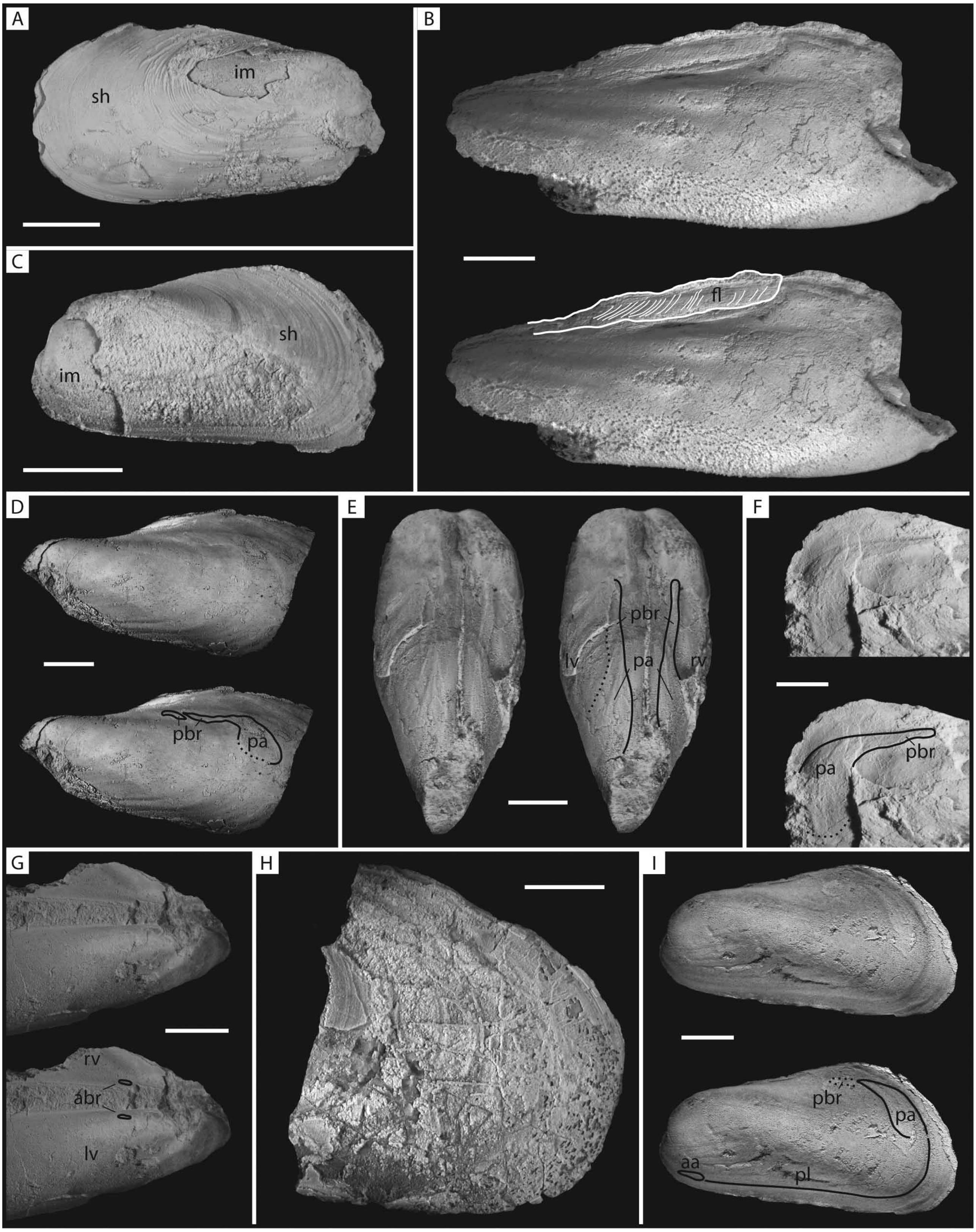
A
im
sh
B
fl
C
sh
im
D
pbr
pa
E
pbr
lv
pa
rv
F
pa
pbr
G
rv
abr
lv
H
I
pbr
pa
aa
pl

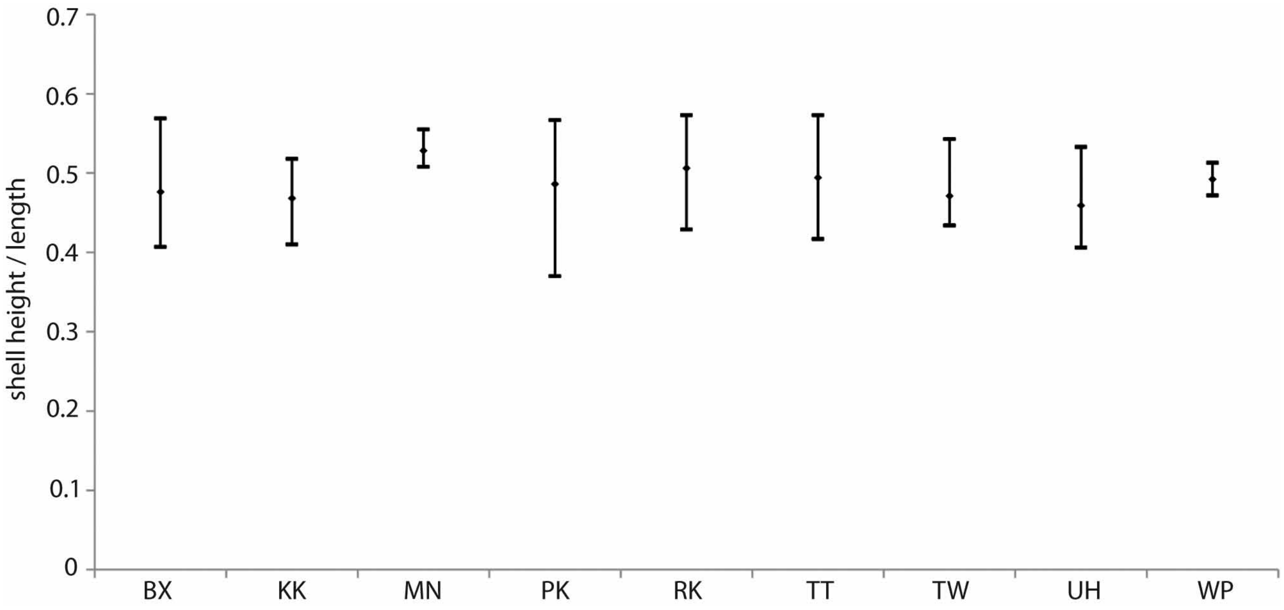

FIGURE 7. Stock chart showing range and mean shell height/length ratios of specimens of *Bathymodiolus heretaunga* **sp. nov.** from each of the study localities. BX: Bexhaven; KK: Karikarihuata; MN: Moonlight North; PK: Puketawa; RK: Rocky Knob; TT: Totaranui; TW: Tauwhareparae; UH: Ugly Hill; WP: Waipiro.

Etymology. The Māori name for Hawke's Bay, a region of New Zealand throughout which localities bearing fossils of this species are found; used as a noun in apposition.

Diagnosis. Shell rather small for group (L up to 95.4 mm), highly variable in shape; umbones situated at 5–14% shell length; umbonal region rather pronounced, angulated; anterior margin broadly rounded in some immature specimens; ventral margin slightly concave in some adult specimens, convex in immature specimens.

Description. Shell rather small for group (L up to 95.4 mm, H up to 35.0 mm, I up to 27.9 mm), elliptical in immature specimens, modioliform in adult specimens (some specimens cuneiform), essentially equivalve, rather thin (usually not preserved or expressed only in flaky patches), highly variable in shape but generally becoming slightly more elongate with growth, adult (L ≥ 38 mm) H/L = 0.37–0.57 (mean = 0.48), smaller specimens with H/L = 0.41–0.57 (mean = 0.50), of which small specimens (L < 15 mm) notably stouter with H/L = 0.44–0.57 (mean = 0.53). Umbones subterminal, prosogyrate, anterior, situated at 5–14% shell length,

FIGURE 6. Various shell features observed upon specimens of *Bathymodiolus heretaunga* **sp. nov.** Scale bar is 5 mm. A. Paratype TM8733, right valve, showing strongly rugose growth lines in medial portion. B. Specimen L4575, left valve internal mould, showing well preserved fibrous layer of the ligament. Original photograph (top) vs. highlighted ligamental area and striations (bottom). C. Specimen L4556, left valve, showing well preserved posterodorsal shell. D. Specimen L4515, left valve internal mould, showing faint scars of posterior adductor and posterior byssal retractor complex. Original photograph (top) vs. highlighted muscle scars (bottom). E. Specimen TM8707, anterodorsal view, showing paired scars of posterior adductor and posterior byssal retractor complex. Original photograph (left) vs. highlighted muscle scars (right). F. Specimen TM8707, posterodorsal portion of right valve, showing the posterior adductor scar united with scar of the posterior byssal retractor complex from the lateral perspective. Original photograph (top) vs. highlighted muscle scars (bottom). G. Specimen TM8745, anterodorsal portion of internal shell, showing paired scars of the anterior byssal retractors. Original photograph (top) vs. highlighted muscle scars (bottom). H. Specimen L4516, posterior portion of left valve, showing byssal attachment scars across shell surface. I. Specimen L4555, left valve, showing scars of anterior and posterior adductors joined by faint pallial line, and faint scars of the posterior byssal retractor complex extending from the anterodorsal tip of the posterior adductor. Original photograph (top) vs. highlighted scars (bottom). aa: scar of anterior adductor; abr: scar of anterior byssal retractor; fl: fibrous layer of ligament; im: internal mould; lv: left valve; pa: scar of posterior adductor; pbr: scar of posterior byssal retractor complex; pl: pallial line; rv: right valve; sh: shell.

in most specimens 6–11%, placement consistent throughout growth; umbonal region rather pronounced and angulated, especially in smaller specimens, becoming more rounded and flattened with growth, covering ca. 15–20% of dorsal length in adult, less in juveniles. Anterior portion of shell short, slightly protrusive in some specimens. Anterior margin narrowly rounded, broadly rounded in some juvenile to half-grown specimens; dorsal margin strongly convex in smallest specimens, gradually becoming less convex with growth, more or less straight in largest specimens; posterodorsal corner usually weakly to strongly angular, broadly rounded in some specimens, marking point of greatest valve height at ca. 70–80% along shell length from anterior margin, only just in posterior in some early juvenile specimens; posterior margin broadly rounded, evenly in some specimens but typically sloping towards the ventral margin; ventral margin rather strongly convex in smallest specimens, becoming weakly convex to nearly straight in half-grown specimens, developing gentle concavity centred just in anterior in adult specimens or remaining more or less straight, in some specimens weakly to moderately convex in posterior third, especially in specimens in which concavity forms. Broadly rounded ridge runs from umbonal region, opening out to posteroventral and ventral margins, becoming obsolete before ventral margin, persisting to posteroventral margin in most specimens. External surface with irregular, fine, well developed commarginal growth lines and waves, rather strongly rugose medially in some specimens (Fig. 6A); growth waves and rugae typically rather strongly reflected on interior, especially in posterior and ventral portions. Hinge and ligament plate unknown. Ligament extending over ca. 85–90% of dorsal margin, running from beaks to in front of posterodorsal corner, terminating in moderately gentle taper. Subligamental ridge typically faint, strong in some specimens, running roughly parallel to ligament from near beak, becoming obsolete at 50–80% ligament length, visible from ventral but not lateral view. Muscle scars strongly impressed to faint, but generally poorly preserved; anterior adductor scar small, oval to elongate oval, located directly below beak close to anteroventral margin; posterior adductor scar medium to large, oval (long axis roughly parallel to posterodorsal margin), contiguous anterodorsally with posterior byssal retractor complex; anterior byssal retractor scar (known only from one specimen) small, oval, located in posterior of umbonal cavity, visible from ventral but not lateral view; posterior byssal retractors form long, thin, continuous scar complex, united with anterodorsal boundary of posterior adductor scar and running anteriorly (also slightly dorsally) in direction towards umbones, terminating at roughly middle of shell length; pallial line indistinct, running between posteroventral boundaries of anterior and posterior adductors, roughly parallel to ventral and posteroventral margins. Larval shell unknown.

Remarks. The new species is identified as a bathymodioline owing to its occurrence at hydrocarbon seep sites and the modioliform shell shape and size. It is assigned to the *B. childressi* clade mainly because of the scar of the posterior byssal retractors, which form a continuous scar united with the posterior adductor, reflecting the multibundle posterior byssal retractor complex diagnostic of modern species of this clade. This key feature distinguishes it from members of the *B. aduloides* and *B. thermophilus* clades, which have well separated anterior and posterior portions of the posterior byssal retractor. The new species can also be assigned to the *B. childressi* group (within the *B. childressi* clade) with some confidence. Each of the diagnostic characters of this group are satisfied in that the shell is small (range is small to rather large), the umbones are subterminal to almost terminal, and the anterior byssal retractor scar is located in the posterior part of the umbonal cavity. The only criterion that is not met precisely is the anterior margin, which is always narrowly rounded in the definition of the *B. childressi* group, but is broadly rounded in some immature specimens of *B. heretaunga*, although narrowly rounded in most specimens. There also are key features that exclude *B. heretaunga* from the other groups of the clade. The shells are too small and stout for the *B.* (*s. l.*) *edisonensis*, *B.* (*s. l.*) *tangaroa* and *Gigantidas* groups, and the position of the anterior byssal retractor scar is different from each. The new species cannot be placed in the *B.* (*s. l.*) *japonicus* group, which consists solely of *B. japonicus* Hashimoto and Okutani, 1994, because this species has the anterior byssal retractor scar located in the anterior portion of the umbonal cavity, and its anterior margin is not narrowly rounded in adult specimens. The subterminal umbonal placement of *B. heretaunga* eliminates inclusion within the *B.* (*s. l.*) *hirtus* group, which contains species with umbones that protrude beyond the anterior margin of the shell. The new species is introduced as the smallest member of the *B. childressi* group, the largest specimen of *B. heretaunga* being 15% smaller than the next smallest described species, *B.* (*s. l.*) *mauritanicus* Cosel, 2002.

Bathymodiolus heretaunga has a quite distinct H/L ratio throughout ontogeny compared to any other member of the group, or for that matter the clade. Within the *B. childressi* group, the H/L ratio of the new species is closest to *B. childressi* Gustafson, Turner, Lutz and Vrijenhoek, 1998 but it is more variable, becoming more elongate when fully grown, and *B. mauritanicus* and *B.* (*s. l.*) *platifrons* Hashimoto and Okutani, 1994 are yet stouter and less variable than *B. heretaunga*. *Bathymodiolus heretaunga* has a rather thin shell like *B. childressi*, but in *B. mauritanicus* and *B. platifrons* the shell is thick and solid. Immature specimens of the new species never develop concavity in the ventral margin unlike *B. childressi*, and ventral concavity is less marked in adult specimens than in *B. mauritanicus*. The umbones are situated more terminally in the other three species of the group than in the new species, which results in a more protrusive anterior portion of the shell in *B. heretaunga*. The umbones also are far more prominent and angulated in *B. heretaunga* than in any other species of the group. The ligament extends over a greater portion of the dorsal margin in *B. heretaunga* than in *B. childressi*, and ends in a moderate taper like *B. childressi* but unlike *B. mauritanicus* and *B. platifrons*, in which it ends abruptly. The subligamental ridge runs beneath the ligament for a similar length to *B. mauritanicus*, but is only visible from the ventral perspective, whereas it is visible from both ventral and lateral views in *B. mauritanicus*. The subligamental ridge also is only visible from the ventral view in *B. platifrons*, however it is typically more distinct in this species. The muscle scars of the new species are similar in size and location to the other species of the group, although they are always indistinct in *B. childressi*, but may be well impressed in *B. heretaunga* (Fig. 6D–F). The new species is most similar to the fossil Japanese species *B. akanudaensis*, with which it shares a similar lateral profile, but *B. akanudaensis* shows a lesser tendency towards elongation with growth, is generally more strongly inflated than *B. heretaunga*, and has slightly more terminal umbones. *B. akanudaensis* also is apparently less variable, and confirmed specimens of the Japanese fossil species have not been observed to reach as large a size as *B. heretaunga*. Furthermore, features of the internal shell of *B. akanudaensis* are unknown, and the muscle scars were a key factor in deciding the placement of *B. heretaunga*, therefore comparison on this important basis is impossible.

Although the majority of *B. heretaunga* specimens are small, occasionally anomalously large specimens have been collected, especially from Tauwhareparae and Totaranui (Table 4). These larger specimens are herein assigned to the same variable new species as the smaller ones on the basis of population-level variation, but it may be that larger specimens from these sites represent a different species. Speciation cannot be confirmed because details of features necessary for species-level identification are unavailable from the collected specimens. This size distribution pattern is also seen in collections of *B. akanudaensis* and unconfirmed larger mussel specimens from the same deposits in Central Japan, with the bulk of specimens of confirmed *B. akanudaensis* being relatively small but the larger mussel specimens sometimes reaching over 100 mm in length and being rather more elongate. Work on the taxonomic relationship among these differently sized specimens is ongoing (T. Nobuhara, pers. comm. 2009). Other intra-site variations also are recognized among the specimens of *B. heretaunga* of this study, again herein regarded as population-level differences in lieu of further specimen collection and establishment of important species-level identifying features. Some of the larger specimens from Bexhaven have more markedly concave ventral margins, and appear to develop one or two moderately strong ridges that run from the umbonal region posteriorly, but this is only observed in three specimens. Some specimens from the type locality Puketawa appear to have the umbones situated less anteriorly, with a more bean-shaped form. They more strongly resemble the shell shape of species of *Adipicola* Dautzenberg, 1927, but there is not enough diagnostic detail in the specimens available for confirmation of this placement. Morphometric data of Puketawa specimens also reveal them to be the least divergent from the “typical” size and shape of *B. heretaunga* of any site population. Finally, specimens from Ugly Hill, the best-sampled of the southern hydrocarbon seep sites, generally appear to have a more cuneiform overall shape, formed by a more pronounced and narrowly rounded posterodorsal corner, although two Ugly Hill specimens provide muscle scar features that are consistent with others from the northern sites (Fig. 6H), and are more confidently regarded as conspecific.

Each of the sites that yielded specimens with suspected population variations also contained specimens that were morphologically close to others sites, suggesting an intra- and inter-site spectrum of shape and size that does not lend itself to separating species easily, especially because of the prevalently poor to moderate preservational condition of the specimens. Principal component analysis of shell height, length, and umbonal placement in those specimens that were preserved well enough for quantitative analysis also did not yield any obvious inter-site patterns (data not shown). The ranges and means of shell height/length ratios of specimens were compared between sites and shown to have considerable overlap, even where the sample data set was quite small and with more potential for anomaly (Fig. 7). The unsuccessful statistical and morphometric attempts to isolate clear variations in shell shape and size between and within sites support the decision to erect a single, variable species until such time as further evidence may prove otherwise.

TABLE 5. Shell height/length ratios of selected specimens of *Bathymodiolus heretaunga* **sp. nov.**, calculated and divided by site.

Site	Mean	SD	n
Bexhaven	0.476	0.045	18
Karikarihuata	0.468	0.034	11
Moonlight North	0.528	0.024	3
Puketawa	0.496	0.035	12
Rocky Knob	0.506	0.037	95
Tauwhareparae	0.471	0.036	10
Totaranui	0.494	0.042	43
Ugly Hill	0.459	0.040	15
Waipiro	0.492	0.029	2

Genus *Gigantidas* Cosel and B. Marshall, 2003

Gigantidas Cosel and B. Marshall, 2003: 37. Type species (by original designation): *Gigantidas gladius* Cosel and B. Marshall, 2003.

Discussion. Of the groups of vent and seep mussels that have been established, *Gigantidas* has the most distinctive features, including shell elongation and shape, as well as in the attachment of the anterior byssal retractor directly behind the anterior adductor in front of the umbones, rather than in the posterior of the umbonal cavity (Cosel and Janssen 2008).

Species *Gigantidas coseli* Saether, Little, Campbell, Marshall, Collins and Alfaro sp. nov.

(Figs. 4B, C, 8–10, 17)

?Mytilid closely resembling *Idasola* Beu & Maxwell, 1990.
?*Bathymodiolus* n. sp. B Collins, 1999.
Group 3 (G3) Collins, 1999.
Large, curved, elongate fossil form similar to *Gigantidas* Campbell *et al.*, 2008.
Bathymodioline bivalves Saether *et al*., 2010.

Holotype. Specimen L4203 (Figs. 8A.6, B.1–4), adult, UOA.

Type locality. Moonlight North (Y16/f1054), Hawke's Bay, North Island, New Zealand; Waiauan (Late Middle Miocene–Earliest Late Miocene) hydrocarbon seep carbonate.

Paratypes. Eight moderately to well preserved small to large specimens. One small, TM8750 (Fig. 8A.2), one medium sized, TM8749 (Figs. 9C, D), from Bexhaven (Y16/f0566); three large, L4560, L4210, L4213, from Moonlight North (Y16/f1033, Y16/f1054); one small, L4204 (Fig. 8A.1), one medium sized, L4209 (Fig. 9E), from Rocky Knob; one medium sized, L4215 (Fig. 8A.4), from Tauwhareparae. All specimens at UOA, two borrowed from GNS. See Table 6 for dimensions.

FIGURE 8. Growth series and holotype of *Gigantidas coseli* **sp. nov.** A. Diagnostic lateral views of left and right valves to show growth series. Scale bar is 20 mm. A.1. Paratype L4204. A.2. Paratype TM8750. A.3. Specimen L4563. A.4. Paratype L4215. A.5. Specimen L4561. A.6. Holotype L4203. A.7. Specimen L4211. B. Diagnostic views of holotype L4203. Scale bar is 10 mm. B.1. Anterior view. B.2. Dorsal view. B.3. Lateral view of left valve. B.4. Lateral view of right valve.

Other material. 22 poorly to moderately preserved small to large specimens: one from Bexhaven (Y16/f1032); 14 from Moonlight North (Y16/f1033, Y16/f1054); one (tentatively assigned) from Puketawa (Y16/f0580), four from Rocky Knob (Y16/f1036, Y16/f1043, Y16/f1047), two from Turihaua (Y18/f0372). All specimens at UOA, three borrowed from GNS. See Appendix I for dimensions and specimen data.

Etymology. Named for Dr. Rudo von Cosel, a leading researcher in vent and seep mussel taxonomy.


A
apb
ppb
pa
pl
B
pa
C
ppb
pa
pl
D
lig
E
rv
lv
F
sh
fl

Diagnosis. Shell small for genus (L up to 99.0 mm); umbones subterminal, anterior, at 6–18% along shell length; anterior portion rather protrusive anteriorly; ligament ending in gentle taper in adult; subligamental ridge visible from lateral and ventral perspectives; posterior adductor scar moderate in size.

TABLE 6. Selected measurements of specimens of *Gigantidas coseli* **sp. nov.** Italicized values are approximate.

Specimen	Type	A	H	I	L	H/L	L/H	U	Site
L4203	Holotype	9.9	25.2	23.4	92.3	0.27	3.66	12%	MN
TM8749	Paratype	4.7	15.1	*14.6*	55.8	0.27	3.70	8%	MN
TM8750	Paratype	6.1	11.1	9.0	34.8	0.32	3.14	18%	BX
L4560	Paratype	8.8	24.4	*16.8*	77.7	0.31	3.18	11%	MN
L4210	Paratype	11.9	27.6	22.2	91.9	0.30	3.33	13%	MN
L4213	Paratype	*11.4*	23.3	*26.0*	91.3	0.26	3.92	*12%*	MN
L4204	Paratype	*2.5*	7.7	6.2	22.1	0.35	2.87	*11%*	RK
L4209	Paratype	6.1	14.9	13.0	49.4	0.30	3.32	12%	RK
L4215	Paratype	7.1	17.5	16.2	*61.0*	*0.29*	*3.49*	*12%*	TW

Description. Shell small for genus (L up to 99.0 mm, H up to 34.0 mm*, I up to 27.0 mm), aduliform, rather thin (usually not preserved or expressed only in flaky patches), slender, becoming more elongate with growth, juvenile (L < 40 mm) H/L = 0.32–0.39, I/L = 0.26–0.34, adult H/L reaching 0.23, I/L reaching 0.18, equivalve, some specimens with valves slightly twisted against one another with left–right sense along anteroposterior axis (Fig. 8B.2). Umbones subterminal, prosogyrate, anterior, in most specimens at 11–13% shell length throughout growth, in some becoming further anterior with increasing size, position more variable in smaller specimens than in larger specimens; umbonal region moderately elongated, moderately pronounced in adult, more angulated and distinct in juveniles, covering ca. 20–25% of dorsal length in adult, less in juveniles. Posterior angulation running from umbones to posterior end of ventral margin, becoming stronger with growth, somewhat sharply defined internally, more rounded externally, forming widest point of shell at about mid-length; in dorsal view, posterior angulation development causes increasing central bulging of shell with growth, tapering to posterior margin; much smaller anterior angulation runs from umbones to anterior margin, forming secondary anterior bulge in dorsal view, area between bulges slightly constricted in some of largest specimens; bulges less apparent in smaller specimens, which appear more uniformly fusiform in dorsal profile. Anterior portion of shell rather protrusive anteriorly. Anterior margin somewhat narrowly and evenly rounded; dorsal margin nearly straight in very small specimens, becoming gently convex in half-grown specimens to rather convex in fully grown specimens; posterodorsal corner at point of greatest valve height, broadly rounded, indistinct to weakly angulated; posterior margin broadly and unevenly rounded, sloping ventrally; ventral margin nearly straight to weakly and more or less evenly convex in juvenile,

FIGURE 9. Various shell features observed upon specimens of *Gigantidas coseli* **sp. nov.** A. Specimen L4559, left valve, showing pallial line and separated anterior and (very faint) posterior portions of posterior byssal retractor scar. Original photograph (left) vs. highlighted scars (right). Scale bar is 5 mm. B. Specimen L4562, posterior portion of internal right valve, showing growth lines within the moderate-sized posterior adductor muscle scar. Original photograph (left) vs. highlighted muscle scars (right). Scale bar is 10 mm. C, D. Paratype TM8749. C. Posterior adductor scar and posterior portion of pallial line on internal left valve of half-grown shell. Original photograph, oblique lateral view (left) vs. highlighted scars, lateral view (right). Scale bar is 5 mm. D. Oblique dorsal view of right valve, showing posterior tapering condition of ligament. Original photograph (top) vs. highlighted ligamental impression (bottom). Scale bar is 10 mm. E. Paratype L4209, close up anterior view of the umbones showing details of the early shell. F. Specimen L4568, dorsal area of right valve, showing well preserved striations of the fibrous layer of the ligament. Scar bar is 2 mm. apb: scar of anterior part of posterior byssal retractor; fl: fibrous layer of ligament; lig: ligament; lv: left valve; pa: scar of posterior adductor; pl: pallial line; ppb: scar of posterior part of posterior byssal retractor; rv: right valve; sh: shell.

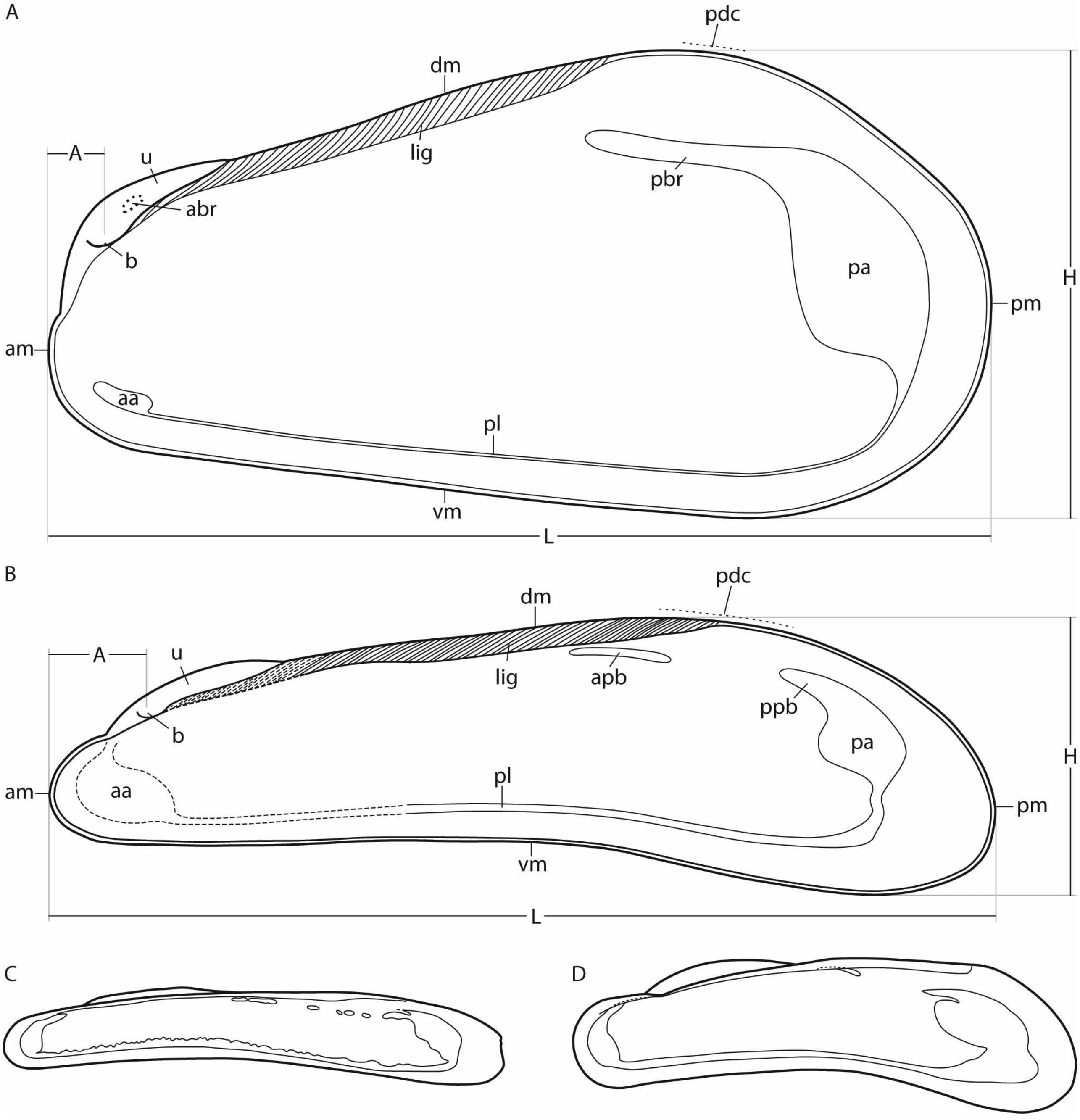

FIGURE 10. Sketches of idealized internal right valves of adult specimens of *Bathymodiolus heretaunga* **sp. nov.**, *Gigantidas coseli* **sp. nov.**, and the two named modern species of *Gigantidas* Cosel and B. Marshall, 2003. Not to scale. A. *B. heretaunga*. B. *G. coseli*. C. *Gigantidas gladius* Cosel and B. Marshall, 2003. D. *Gigantidas horikoshii* Hashimoto and Yamane, 2005. A and B based on holotype shell shapes but constructed as composites from details observed in several specimens for both new species. Features unknown in *G. coseli* are estimated from those typical of the genus, and are drawn as dashed lines. C and D modified from Cosel and Marshall (2003: fig. 33) and Hashimoto and Yamane (2005: fig. 9) respectively. A: shell anterior length; aa: scar of anterior adductor; abr: scar of anterior byssal retractor; am: anterior margin; apb: scar of anterior part of posterior byssal retractor; b: beak; dm: dorsal margin; H: shell height; L: shell length; lig: ligament; pa: scar of posterior adductor; pbr: scar of posterior byssal retractor complex; pdc: posterodorsal corner; pl: pallial line; pm: posterior margin; ppb: scar of posterior part of posterior byssal retractor; u: umbo; vm: ventral margin.

specimens), strongly concave in adults, rather strongly convex along posterior third, straight (typically) or weakly convex in anterior quarter below umbo. External surface with irregular, well developed commarginal growth lines and waves; growth waves weakly reflected on interior, especially towards margins, strongest in posteroventral portion. Hinge and ligament plate unknown. Ligament extending over ca. 80–90% of dorsal margin, running from beaks to in front of posterodorsal corner, terminating posteriorly in gentle taper. Subligamental ridge well developed, running from behind beaks, becoming obsolete at 70–100% ligament length in direction diverging from dorsal margin towards point about two-thirds up on posterior margin, clearly visible from lateral perspective. Muscle scars faint (generally poorly preserved, known principally from three specimens, Figs. 9A–C); anterior adductor and anterior byssal retractor scars unknown; posterior adductor scar of moderate size, situated at two-thirds of valve height in dorsal half, posterior limb rounded, united anterodorsally with posterior scar of posterior byssal retractor; anterior scar of posterior byssal retractor well separated, preserved in only one incomplete specimen with eroded dorsal margin, making relative position unclear, but roughly beneath third and last quarter of ligament; pallial line more or less parallel with ventral margin, at least in posterior half, anterior portion not preserved in any specimens. Larval shell unknown.

* Measured in an incomplete internal mould comprising the largest posterior portion of any specimen in the collections, which, if assumed to be from a shell of typical overall shape, would reach a length of at least 120–150 mm, especially with consideration of the trend of increasing elongation with growth.

Remarks. *Gigantidas* is a recently erected genus with only two species (both modern) so far described. Although the group is largely based upon anatomical features, several shell characteristics can be used to justify inclusion of the new species there, including shell elongation and overall shape, umbonal placement, position of the posterior adductor muscle scar, fusion of the posterior adductor muscle scar with the posterior scar of the posterior byssal retractor, and the widely separated anterior part of the posterior byssal retractor scar. Of the two modern species, *G. coseli* resembles *G. gladius* in lateral view and *G. horikoshii* in dorsal view. *Gigantidas coseli* is less elongate than *G. gladius* and more elongate than *G. horikoshii*, and the largest specimens of *G. coseli* are significantly smaller than both. The umbones are somewhat more anteriorly placed than in *G. gladius* and *G. horikoshii*. The posterior angulation runs at a steeper angle over the shell than *G. gladius* and *G. horikoshii*, its termination occurring in a more anteroventral shell location. The anterior angulation is less pronounced than *G. gladius*, the dorsal profile with a weaker secondary anterior bulge similar to that of *G. horikoshii*. The anterior part of the shell is less protrusive anteriorly than in *G. gladius* and *G. horikoshii* because of the more anteriorly situated umbones, and the anterior margin is less narrowly rounded than in both *G. gladius* and *G. horikoshii*. The ligament ends in a gentle taper posteriorly in adult *G. coseli*, unlike *G. gladius* in which the termination is abrupt or has a short taper, and *G. horikoshii* in which it is abrupt, although it is weakly tapered in smaller specimens of *G. horikoshii*. The subligamental ridge of *G. coseli* is strong like in *G. gladius* and *G. horikoshii*, but oriented more divergently from the dorsal margin, allowing it to be seen from the lateral perspective, unlike in *G. gladius* and *G. horikoshii*, in which it is only visible from the ventral perspective. The posterior adductor scar is smaller relative to the shell compared with that of *G. gladius* and *G. horikoshii*. Morphometric analysis supports a closer relation of the new species to *G. gladius* than *G. horikoshii*, with the ontogenetic height vs. length curve of the smaller *G. coseli* appearing to align with that of the larger *G. gladius* (Fig. 11). The growth curve of *G. horikoshii* (Fig. 11) is quite distinct from those of the other two species, clearly diverging from that of *G. coseli* already at the stage of quarter-grown specimens (L = 40–50 mm), and showing consistently less tendency toward elongation with growth through to the fully grown stage.

Gigantidas coseli represents the first record of a formally described and named species in this genus from a hydrocarbon seep environment, with all reports of modern named species having so far been from hydrothermal vent sites in the Pacific Ocean. However, up to three undescribed species have been reported from seep environments off Japan and New Zealand (Fujita *et al.* 2009; Baco *et al.* 2010; Table 2), and there are several other species within the *B. childressi* clade that are known only from hydrocarbon seep sites, including those from geographically close regions in the SW Pacific, and two species in the clade (*B. japonicus* and *B. platifrons*) are recorded from both hydrocarbon seep and hydrothermal vent environments (Table 1).

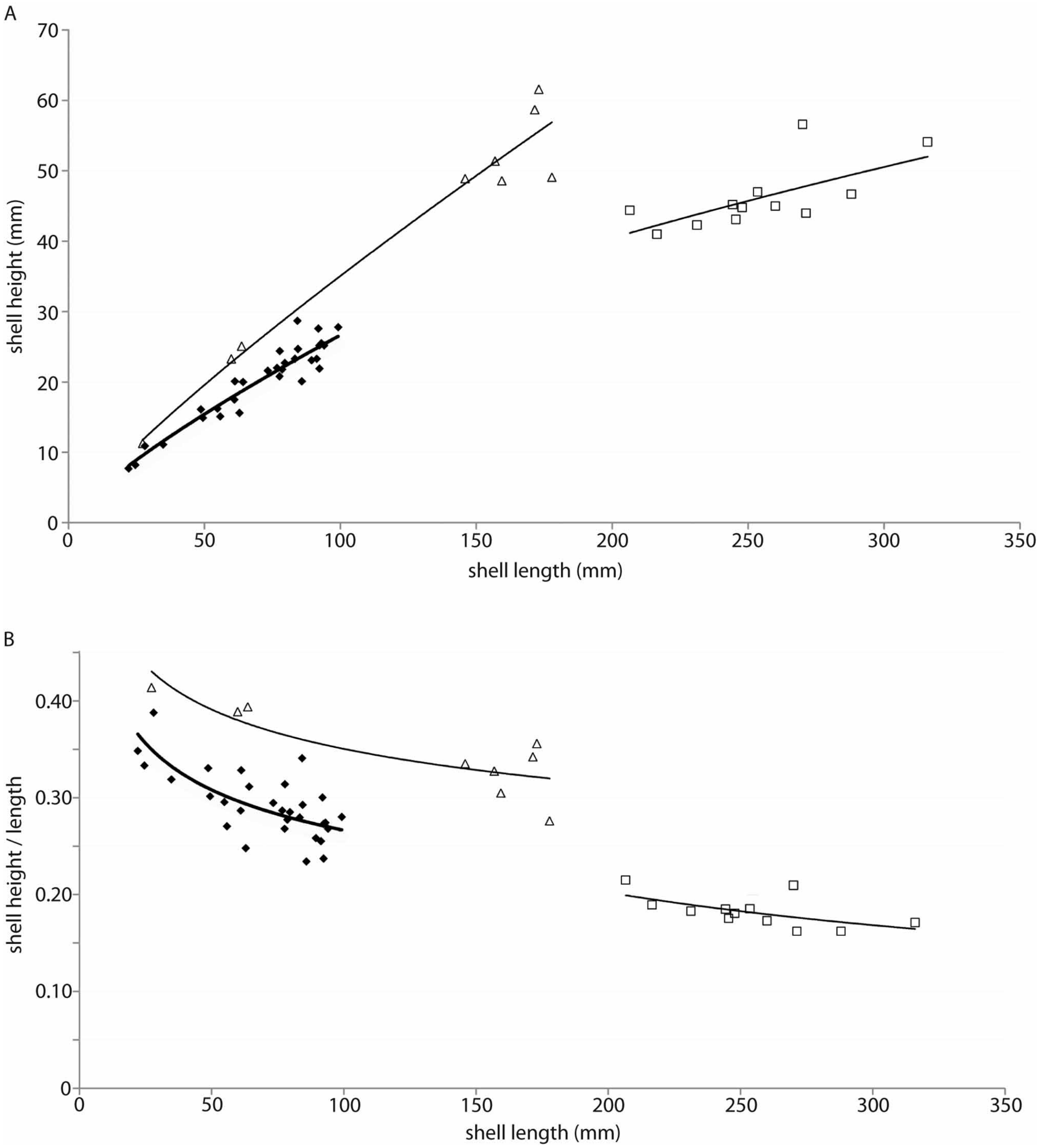

FIGURE 11. Scatter plot with lines of best fit showing ontogenetic changes in shell height vs. shell length (A) and shell height/length ratio vs. shell length (B) in specimens of *Gigantidas coseli* **sp. nov.** and its modern congeners. ◆: *G. coseli*; □: *G. gladius* Cosel and B. Marshall, 2003; △: *G. horikoshii* Hashimoto and Yamane, 2005.

Discussion

Mode of life and preservation in New Zealand fossil hydrocarbon seep mussels

It is rare to find mussel specimens at New Zealand fossil hydrocarbon seep sites in life position. A typical occurrence consists of a dense shell hash with few, if any, intact valves within individual carbonate boulders or blocks. It is also relatively common to encounter articulated, randomly oriented specimens in close association and, in places, clusters of shells. Adjacent in-situ specimens have been observed with a preferred orientation (Fig. 4B) and other well preserved specimens show byssal attachment scars in the posterior shell portions (Fig. 6H). These lines of evidence allow interpretation of likely mode of life in New Zealand fossil hydrocarbon seep mussels, and inference of several phases in their early taphonomic history. Initially, living animals likely attached byssally to carbonate hardgrounds formed at the sea floor (e.g. Campbell *et al.* 2010, fig. 7H). Next, clusters of mussels were built up by attaching to the posterior areas of shells that colonized the hardground. As population densities increased, some mussels were crowded out, fell off their attachment sites, and became disarticulated and fragmented. Rapid carbonate mineralization then encased the broken shells to preserve a strongly indurated shell hash (cf. Campbell *et al.* 2010, fig. 7J). Rarely, a rapid obrution event preserved the shells in life position or, more typically, shifted them slightly to create parautochthonous assemblages of articulated, randomly oriented specimens (Fig. 4C).

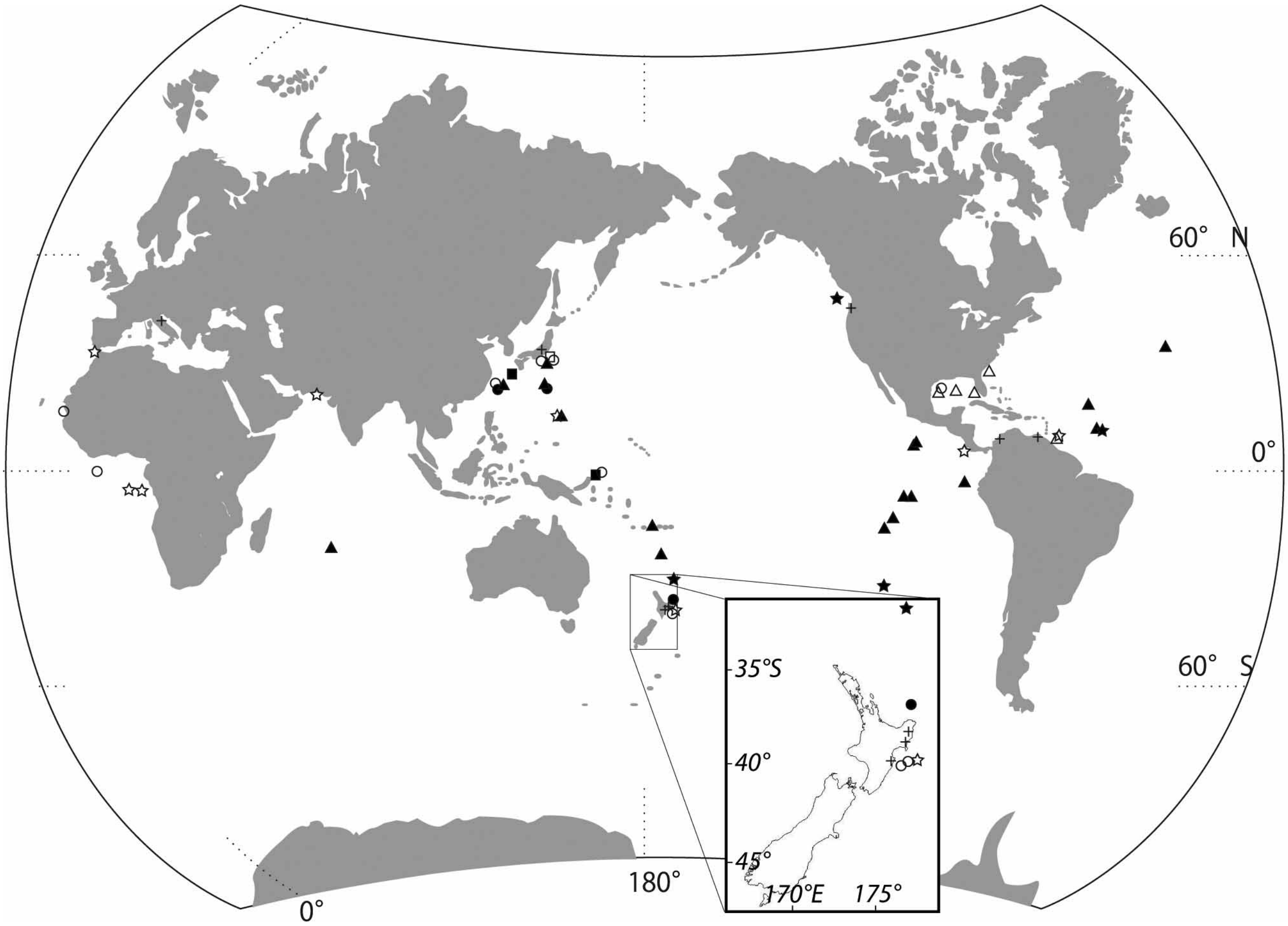

FIGURE 12. Map to show global distribution of vent–seep mussel species. Inset: fossil and modern occurrences of New Zealand vent–mussel taxonomy. ■: *Bathymodiolus aduloides* clade; ●: *Bathymodiolus childressi* clade; ▲: *Bathymodiolus thermophilus* clade; ★: species still in open nomenclature; +: fossil occurrence. Closed and open symbols indicate modern hydrothermal vent and hydrocarbon seep environments respectively.

Palaeobiogeographic patterns in vent and seep mussels

The *B. childressi* clade—constituting 12 modern described species plus one subspecies (Table 1) and three fossil species (the two described herein and *B. akanudaensis* from a Miocene hydrocarbon seep in central Japan [T. Nobuhara, pers. comm. 2009])—has a global distribution at both hydrocarbon seeps (at least 10 distinct regions) and hydrothermal vents (three distinct regions) in the western Pacific, Gulf of Mexico, and eastern Atlantic (Table 1; Fig. 12). Its distribution may be extended to include the northern Indian Ocean when an undescribed species from the Makran accretionary prism is given formal treatment, as initial observations suggest it will be placed within this clade (R. von Cosel, pers. comm. 2009). The *B. thermophilus* clade, which contains 10 modern described species, is somewhat more widely reported from at least 15 distinct hydrothermal vent regions, most of which are in the Pacific, and at least five distinct hydrocarbon seep regions, most of which are in the Gulf of Mexico (Table 1; Fig. 12). The *B. aduloides* clade contains only two species, *B. aduloides* itself, known only from hydrothermal vents and hydrocarbon seeps off Japan, and *Bathymodiolus* (*s. l.*) *manusensis* Hashimoto and Furuta, 2007, known only from hydrothermal vents off Papua New Guinea and possibly hydrothermal vents or hydrocarbon seeps off New Zealand (Fujita *et al.* 2009). All reports of modern vent and seep mussels are from localities within 48° of latitude (47°56'N–40°26'S). Only three fossil hydrocarbon seep mussel species have been assigned to a particular clade, all within the *B. childressi* clade (see above). Extant members of the *B. childressi* clade also are present in the modern offshore hydrocarbon seeps or hydrothermal vents associated with both of these uplifted and exhumed fossil hydrocarbon seep regions, with *B.* (*s. l.*) *hirtus* Okutani, Fujikura and Sasaki, 2004, *B. japonicus*, *B. platifrons*, and *B.* (*s. l.*) *securiformis* Okutani, Fujikura and Sasaki, 2004 occurring off Japan, and *B.* (*s. l.*) *tangaroa tangaroa* Cosel and B. Marshall, 2003 and *G. gladius* found off the north-east coast of New Zealand's North Island. A geographic subspecies of *B. tangaroa*, *B.* (*s. l.*) *tangaroa tuerkayi* Cosel and Janssen, 2008, also occurs in the SW Pacific at methane seeps on the Edison Seamount off Papua New Guinea. *B.* (*s. l.*) *palmarensis* Kiel, Campbell and Gaillard, 2010 is assigned to *Bathymodiolus* (*sensu lato*), but its placement within either of the two *sensu lato* clades, *B. aduloides* or *B. childressi*, is not specified.

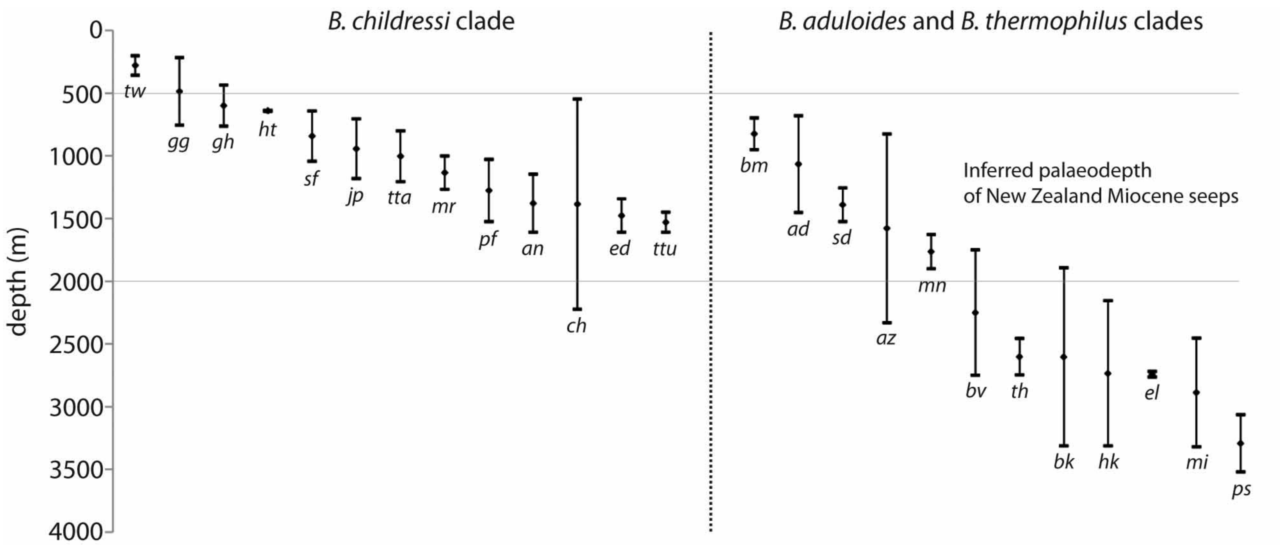

FIGURE 13. Stock chart showing depth ranges of described modern vent–seep mussel species and inferred palaeodepth of New Zealand hydrocarbon seep deposits. Species of the *Bathymodiolus childressi* clade are grouped separately from species of the *B. aduloides* and *B. thermophilus* clades to show the distinct bathymetric distributions of these two species groupings. *ad*: *B. aduloides* Hashimoto and Okutani, 1994; *an*: *B. anteumbonatus* Cosel and Janssen, 2008; *az*: *B. azoricus* Cosel and Comtet in Cosel, Comtet and Krylova, 1999; *bk*: *B. brooksi* Gustafson, Turner, Lutz and Vrijenhoek, 1998; *bm*: *B. boomerang* Cosel & Olu, 1998; *bv*: *B. brevior* Cosel, Métivier and Hashimoto, 1994; *ch*: *B. childressi* Gustafson, Turner, Lutz and Vrijenhoek, 1998; *ed*: *B. edisonensis* Cosel and Janssen, 2008; *el*: *B. elongatus* Cosel, Métivier and Hashimoto, 1994; *gg*: *Gigantidas gladius* Cosel and B. Marshall, 2003; *gh*: *G. horikoshii* Hashimoto and Yamane, 2005; *hk*: *B. heckerae* Turner, Gustafson, Lutz and Vrijenhoek in Gustafson, Turner, Lutz and Vrijenhoek, 1998; *ht*: *B. hirtus* Okutani, Fujikura and Sasaki, 2004; *jp*: *B. japonicus* Hashimoto and Okutani, 1994; *mn*: *B. manusensis* Hashimoto and Furuta, 2007; *mi*: *B. marisindicus* Hashimoto, 2001; *mr*: *B. mauritanicus* Cosel, 2002; *pf*: *B. platifrons* Hashimoto and Okutani, 1994; *ps*: *B. puteoserpentis* Cosel, Métivier and Hashimoto, 1994; *sd*: *B. septemdierum* Hashimoto and Okutani, 1994; *sf*: *B. securiformis* Okutani, Fujikura and Sasaki, 2004; *th*: *B. thermophilus* Kenk and Wilson, 1985; *tta*: *B. tangaroa tangaroa* Cosel and B. Marshall, 2003; *ttu*: *B. tangaroa tuerkayi* Cosel and Janssen, 2008; *tw*: *B. taiwanensis* Cosel, 2008a.

Broadly, modern species of the *B. childressi* clade have been reported from a shallower depth range (200–2222 m) than species of the *B. aduloides* and *B. thermophilus* clades (679–3521 m), although overlap is apparent (Table 1, Fig. 13). This overlap is almost entirely between just five of the 23 bathymodioline (sub)species, only one of which, *B. childressi*, belongs to the *B. childressi* clade. The palaeobathymetry for the New Zealand hydrocarbon seep fossil sites, akin to the ages of the deposits, is poorly constrained. Only two sites have significant micropalaeontological data for inferring likely palaeodepths, Karikarihuata (middle to upper bathyal, or 400–2000 m) and Turihaua (middle bathyal, or 1000–2000 m) (Hayward 1978, 1986; Scott 1985). However, inferences can be made by examining the lithological characteristics of the New Zealand fossil hydrocarbon seep deposits and comparing them to samples from modern New Zealand hydrocarbon seep sites with known depth associations. The northern fossil hydrocarbon seep sites are characterized by greenish-grey microcrystalline carbonates (micarbs), typically layered, and some with a mottled (“oatmeal”; i.e. microbial) fabric, containing strongly indurated fossils, especially mussels and worm tubes (Campbell *et al.* 2008). The southern site lithologies are generally more friable (i.e. less cemented), characterized by a coarser, sandy micarb, and tend to be dominated by lucinid and vesicomyid bivalves (Campbell *et al.* 2008). Modern hydrocarbon seep carbonates have been dredged from the Bay of Plenty and the Hikurangi margin, off eastern North Island, with lithologies comparable to both northern and southern New Zealand fossil hydrocarbon seep lithologies (Lewis and Marshall 1996). Relatively dense, mottled, mussel-rich hydrocarbon seep carbonate, similar to the typical northern New Zealand fossil hydrocarbon seep lithology, was collected from 600 m depth at 38°52’S / 178°32’E on the Hikurangi margin, north of Gisborne (M. Morley, unpublished data). Coarser, brittler, vesicomyid-dominated hydrocarbon seep carbonate also has been collected from several localities on the Hikurangi margin further south, especially from the Rock Garden area (39°59’S / 178°14’N to 40°03’S / 178°14’N) at depths in the range of 610–907 m (Campbell *et al.* 2010), which bears a close resemblance to the lithology of southern New Zealand hydrocarbon seep fossil deposits. In both northern and southern ancient deposits, comparison with modern analogous hydrocarbon seep lithologies suggests that the New Zealand examples formed in relatively shallow, 500–2000 m depth. This broadly correlates with modern depth reports for living species of the *B. childressi* clade (Fig. 13), and is consistent with placement of the New Zealand fossil species within this taxon. To confirm this hypothesis, better depth and age data could be derived from microfossils in mudstones associated with the Miocene hydrocarbon seep carbonates.

Evolutionary patterns in vent and seep mussels

In this discussion, the term “*Bathymodiolus*-group species” is introduced to refer to all species currently assigned to groups within the *Bathymodiolus* clades, both *sensu stricto* and *sensu lato*, as distinct from *Gigantidas*. Size data for undescribed species (Table 7, Fig. 16) are ignored for the purpose of this discussion, as they cannot be considered rigorous until formal descriptive treatment of these species has been undertaken. A possible *Bathymodiolus* species from the Pliocene of central Japan (Nobuhara 2003) also is still only tentatively recognized as a bathymodioline species, with only one specimen known in which details elucidating a clear taxonomic placement are absent, and it is not considered further here.

TABLE 7. Maximum sizes (L_{max}, in mm) reported in vent and seep mussel species, fossil species shaded. Data with asterisks supplied by R. von Cosel (unpublished data); all other data from original descriptions (or for undescribed species, as referenced in the left-hand column of Table 2, except for *B.* sp. GOC Génio *et al.* 2008, provided by L. Génio, pers. comm. 2009). Italicized values are approximate.

Species	L_{max}
B. boomerang	360.0
G. gladius	316.0
B. sp. A	_300_*
B. heckerae	230*
B. tangaroa tangaroa	200.0
B. thermophilus	200*
G. horikoshii	195*

......continued next page

TABLE 7. (continued)

Species	L_{max}
B. sp. IV	190*
B. brooksi	180*
V. insolatus	180*
B. edisonensis	163.6
B. elongatus	156.2
B. brevior	143.5
B. securiformis	135.0
B. sp. B of Olu-Le Roy *et al*., 2007	127*
B. sp. B of Cordes *et al*., 2007	*125**
B. septemdierum	124.0
B. childressi	123.6
B. sp. aff. *puteoserpentis*	123.2
B. tangaroa tuerkayi	120.0
B. azoricus	119.3
B. puteoserpentis	119.0
B. platifrons	115.6
B. mauritanicus	110.0
B. exbrocchii	110.0
B. japonicus	106.2
B. cf. *thermophilus*	105*
B. sp. from Makran	104.5*
B. manusensis	100.8
G. coseli **sp. nov.**	99.2
B. aduloides	96*
B. heretaunga **sp. nov.**	94.7
B. marisindicus	86*
B. hirtus	81.2
B. sp. GOC	66
B. anteumbonatus	60.5
B. akanudaensis	*>60*
T. fisheri	58*
B. taiwanensis	56.0
B. palmarensis	49
B. sp. JdF	20
B. willapaensis	20.0

The known fossil hydrocarbon seep mussels almost always are smaller in size than the described modern forms to which they are most closely associated. In the *Gigantidas* group, *G. coseli* **sp. nov.** is significantly smaller than the two modern species (Fig. 17). No shell dimensional data on juvenile to half-grown specimens of *G. gladius* of a similar size to, or smaller than, the largest *G. coseli* specimens have been published for direct comparison, but Cosel and Marshall (2003) noted that juvenile specimens of *G. gladius* are already similarly slender compared to adult specimens. The apparent alignment of the ontogenetic height vs. length growth curves of specimens of *G. coseli* and large *G. gladius* (Fig. 11) suggests antecedence of *G. coseli* to *G. gladius*,

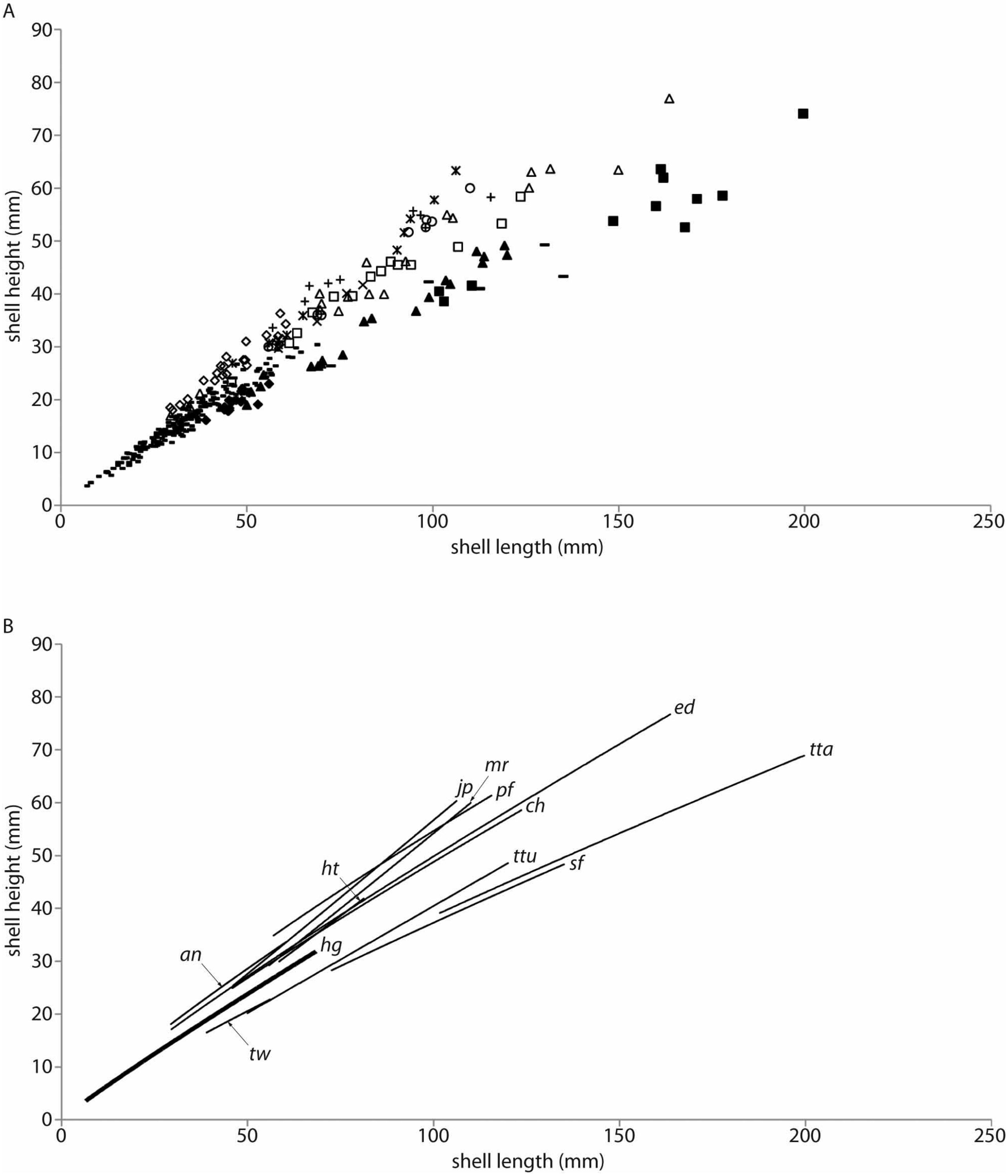

FIGURE 14. Graphs showing ontogenetic changes in shell height vs. shell length in specimens of *Bathymodiolus heretaunga* **sp. nov.** and its modern congeners. A. Scatter plot of raw data. Closed symbols represent species in the *B. tangaroa* group; open symbols are used for other species of the *B. childressi* clade. B. Lines of best fit to show growth curves. ◇: *B. anteumbonatus* Cosel and Janssen, 2008 (*an*); □: *B. childressi* Gustafson, Turner, Lutz and Vrijenhoek, 1998 (*ch*); △: *B. edisonensis* Cosel and Janssen, 2008 (*ed*); ▪: *B. heretaunga* (*hg*); ×: *B. hirtus* Okutani, Fujikura and Sasaki, 2004 (*ht*); ∗: *B. japonicus* Hashimoto and Okutani, 1994 (*jp*); ○: *B. mauritanicus* Cosel, 2002 (*mr*); +: *B. platifrons* Hashimoto and Okutani, 1994 (*pl*); —: *B. securiformis* Okutani, Fujikura and Sasaki, 2004 (*sf*); ◆: *B. taiwanensis* Cosel, 2008a (*tw*); ■: *B. tangaroa tangaroa* Cosel and B. Marshall, 2003 (*tta*); ▲: *B. tangaroa tuerkayi* Cosel and Janssen, 2008 (*ttu*).

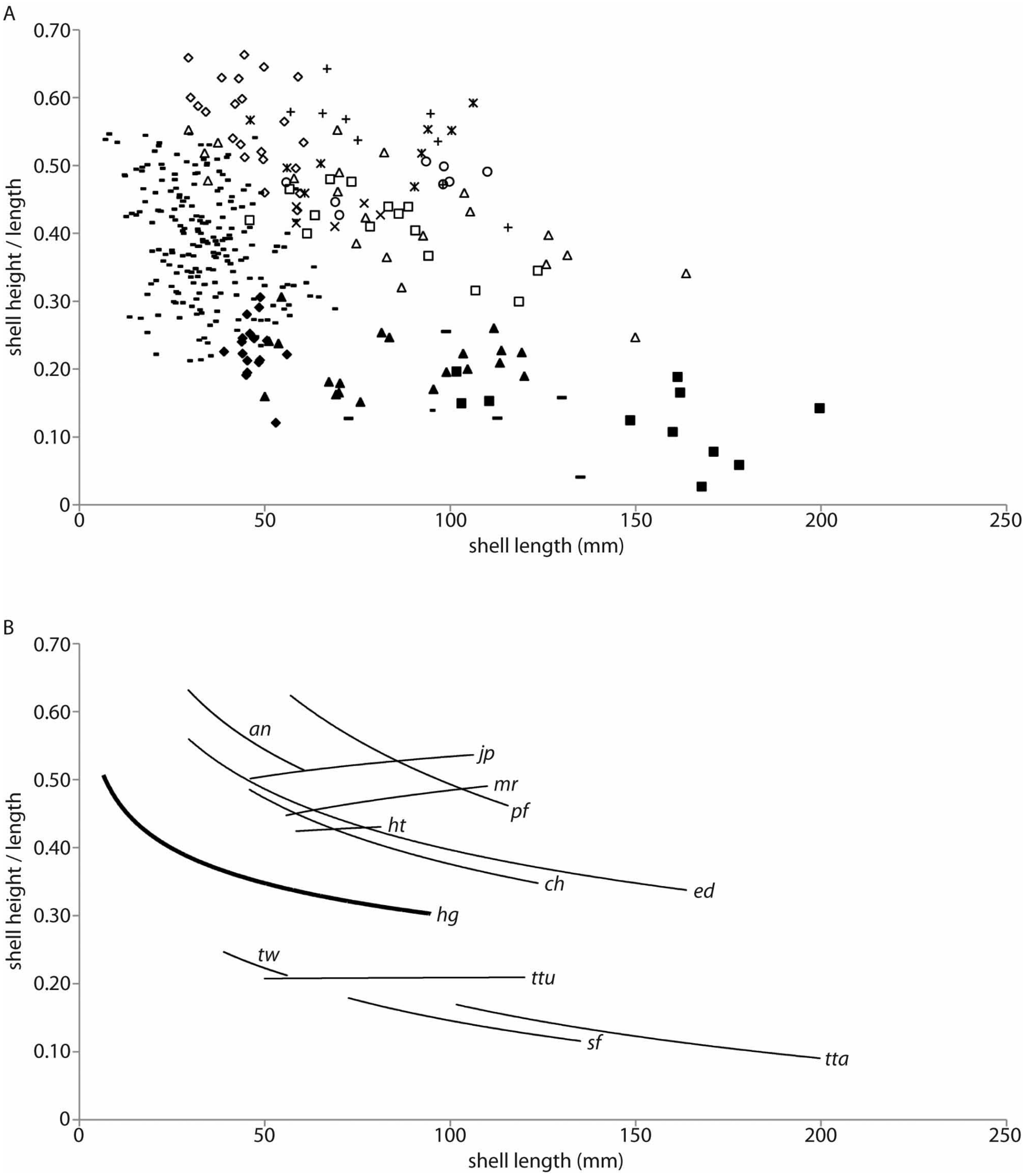

FIGURE 15. Graphs showing ontogenetic changes in shell height/length ratio vs. shell length in specimens of *Bathymodiolus heretaunga* **sp. nov.** and its modern congeners. A. Scatter plot of raw data. Closed symbols represent species in the *B. tangaroa* group; open symbols are used for other species of the *B. childressi* clade. B. Lines of best fit to show growth curves. ◇: *B. anteumbonatus* Cosel and Janssen, 2008 (*an*); □: *B. childressi* Gustafson, Turner, Lutz and Vrijenhoek, 1998 (*ch*); △: *B. edisonensis* Cosel and Janssen, 2008 (*ed*); ▪: *B. heretaunga* (*hg*); ×: *B. hirtus* Okutani, Fujikura and Sasaki, 2004 (*ht*); ✳: *B. japonicus* Hashimoto and Okutani, 1994 (*jp*); ○: *B. mauritanicus* Cosel, 2002 (*mr*); +: *B. platifrons* Hashimoto and Okutani, 1994 (*pl*); —: *B. securiformis* Okutani, Fujikura and Sasaki, 2004 (*sf*); ◆: *B. taiwanensis* Cosel, 2008a (*tw*); ■: *B. tangaroa tangaroa* Cosel and B. Marshall, 2003 (*tta*); ▲: *B. tangaroa tuerkayi* Cosel and Janssen, 2008 (*ttu*).

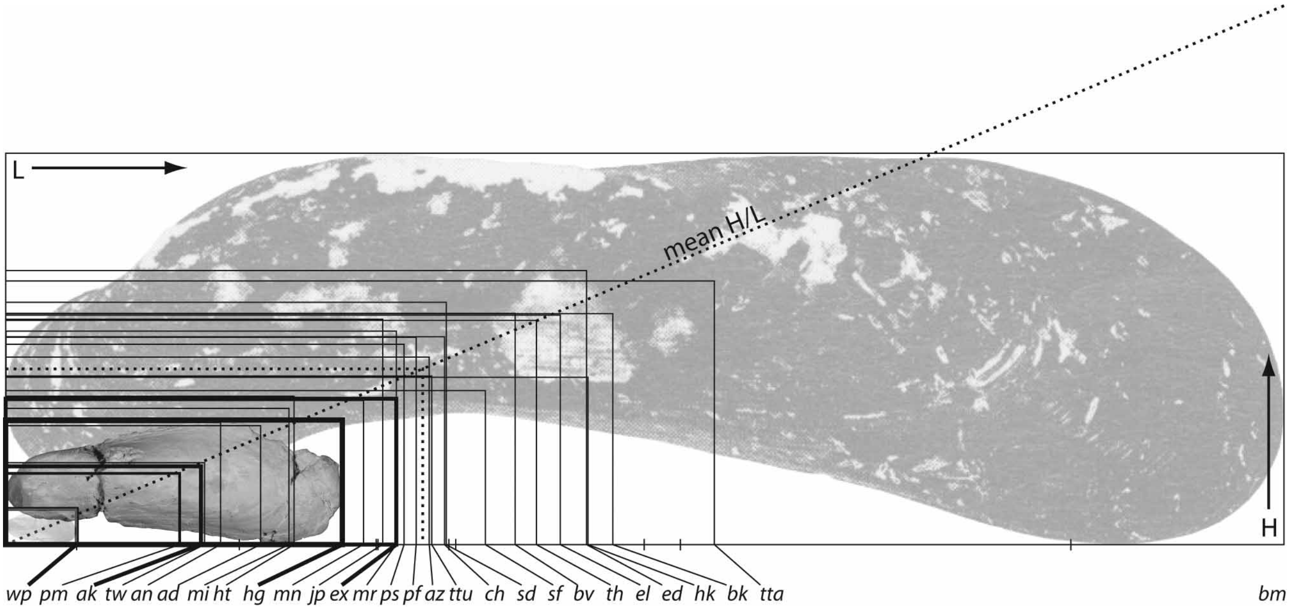

FIGURE 16. Diagram depicting range of relative maximum sizes reported* in species of the genus *Bathymodiolus* Kenk and Wilson, 1985 (*sensu lato* and *sensu stricto*) against the largest specimen of *B. heretaunga* **sp. nov.** (paratype TM8724). Modern species are represented by thin-lined boxes, fossil species by bold-lined boxes. Mean maximum size (H = 49.4 mm, L = 117.3 mm) and H/L ratio (0.44) for genus shown by dashed lines. Tick marks indicate lengths of various undescribed species (see Table 7). Faded background images are holotypes of largest (*B. boomerang* Cosel and Olu, 1998, H = 110.0 mm, L = 360.0 mm) and smallest (*B. willapaensis* (Squires and Goedert, 1991), H = 10.0 mm, L = 20.0 mm) species in the genus. These holotype images are slightly distorted to fill the dimensions of the largest specimen of each species reported, modified from Cosel and Olu (1998: fig. 1) and Squires and Goedert (1991: fig. 2.4). *ad*: *B. aduloides* Hashimoto and Okutani, 1994; *ak*: *B. akanudaensis* (Kuroda, 1931); *an*: *B. anteumbonatus* Cosel and Janssen, 2008; *az*: *B. azoricus* Cosel and Comtet in Cosel, Comtet and Krylova, 1999; *bk*: *B. brooksi* Gustafson, Turner, Lutz and Vrijenhoek, 1998; *bm: B. boomerang* Cosel & Olu, 1998; *bv*: *B. brevior* Cosel, Métivier and Hashimoto, 1994; *ch*: *B. childressi* Gustafson, Turner, Lutz and Vrijenhoek, 1998; *ed*: *B. edisonensis* Cosel and Janssen, 2008; *el*: *B. elongatus* Cosel, Métivier and Hashimoto, 1994; *ex*: *B.? exbrocchii* (Sacco, 1898); H: shell height; *hg*: *B. heretaunga*; *hk*: *B. heckerae* Turner, Gustafson, Lutz and Vrijenhoek in Gustafson, Turner, Lutz and Vrijenhoek, 1998; *ht*: *B. hirtus* Okutani, Fujikura and Sasaki, 2004; *jp*: *B. japonicus* Hashimoto and Okutani, 1994; L: shell length; *mn*: *B. manusensis* Hashimoto and Furuta, 2007; *mi*: *B. marisindicus* Hashimoto, 2001; *mr*: *B. mauritanicus* Cosel, 2002; *pf*: *B. platifrons* Hashimoto and Okutani, 1994; *pm*: *B. palmarensis* Kiel, Campbell and Gaillard, 2010; *ps*: *B. puteoserpentis* Cosel, Métivier and Hashimoto, 1994; *sd*: *B. septemdierum* Hashimoto and Okutani, 1994; *sf*: *B. securiformis* Okutani, Fujikura and Sasaki, 2004; *th*: *B. thermophilus* Kenk and Wilson, 1985; *tta*: *B. tangaroa tangaroa* Cosel and B. Marshall, 2003; *ttu*: *B. tangaroa tuerkayi* Cosel and Janssen, 2008; *tw*: *B. taiwanensis* Cosel, 2008a; *wp*: *B. willapaensis* (Squires and Goedert, 1991).

* Data acquired from published descriptions, where height values also are available for the purpose of this diagram. Cosel (unpublished data) has found greater maximum lengths for *B.aduloides*, *B. brooksi*, *B. heckerae*, *B. marisindicus*, *B. puteoserpentis* and *B. thermophilus* (see Table 7). Goedert *et al.* (2003) reported a possible maximum length of up to 30 mm in a broken specimen of *B. willapaensis*, a 50% longer maximum length than stated in Squires and Goedert (1991), but its identification remains tentative and the maximum verified length is used herein. T. Nobuhara (pers. comm. 2009) provided a possible maximum length for *B. akanudaensis* of over 100 mm, but taxonomic evaluation of the more elongate specimens is still underway, and only verifiable information from Nobuhara *et al.* (2008) and a manuscript plate (T. Nobuhara, unpublished) is used herein.

in that their shells appear to have enlarged (Fig. 17) since the Miocene, and also developed the various other morphological characters discussed above. Of the *Bathymodiolus*-group species, fossil forms constitute the three smallest species described, and all five described fossil species are smaller than both the mean maximum height and mean maximum length of these species (Fig. 16). Amongst *Bathymodiolus*-group species, the largest fossil member, *B.? exbrocchii* (Sacco, 1898), is larger than seven of the 23 described modern (sub)species. *Bathymodiolus heretaunga* is the only fossil mussel among the *Bathymodiolus*-group species that has been assigned to a particular group, as defined by Cosel and Janssen (2008), and it is the smallest member of that group. Fossil *Bathymodiolus*-group species are generally more elongate than modern species of a similar maximum length. Four of the five *Bathymodiolus*-group fossil species are more elongate than the mean H/L ratio of these species—only the smallest, *B. willapaensis* (Squires and Goedert 1991), is stouter—where 10 of the 13 smallest modern species are stouter (Fig. 16). In addition, there is evidence for the steady increase in size of *Bathymodiolus*-group species through time. *Bathymodiolus willapaensis* represents the earliest known (Eocene) occurrence, and is the smallest *Bathymodiolus*-group species. The next smallest member is *B. palmarensis* Kiel, Campbell and Gaillard, 2010, which also is the next oldest (Oligocene). The three other fossil mussels are all of Miocene age, and are the three largest fossil species, although *B.*? *exbrocchii* from Italy and *B. heretaunga* from New Zealand are significantly larger than *B. akanudaensis* from Japan. *Bathymodiolus*? *exbrocchii* has no geographically close modern species for comparison, and is still only tentatively assigned to the group.

Stanley (1973) reviewed the notion of a widespread tendency of animal groups to evolve toward larger physical size, commonly known as Cope's rule, and pointed out that it generally occurs for several main reasons. These include an improved ability to capture prey or ward off predators, greater reproductive success, increased intelligence, better stamina, expanded size range of acceptable food, decreased annual mortality, extended individual longevity, and increased heat retention per unit volume. Much of this hypothesis is based upon mammalian physiology but the pattern is seen in a wide range of animal groups and, in the case of the vent and seep mussels, potential benefits include individual longevity, if modern shells can be assumed to have grown at a similar rate to their fossil counterparts, which is suggested by the similar spacing of their growth lines. Another benefit of greater size may be an increased capacity to harbour microbial endosymbionts for nutrition (shell size often, but not always, correlative with gill size). Generic size benefits may not constitute the only explanations for a perceived evolutionary increase in vent and seep mussel shell size. One driving factor may have been a shift in their mode of life—for example, more Miocene specimens may have been semi-infaunal, like *G. horikoshii* today (Hashimoto and Horikoshi 1989; Hashimoto and Yamane 2005), a life history that generally suits organisms of a smaller size. There may be, for one reason or another, a greater amount of available energy in modern seep habitats than there was in ancient times, perhaps as other organisms adapt successfully to life in these harsh environments, allowing modern species to grow more quickly, and over a longer lifespan.

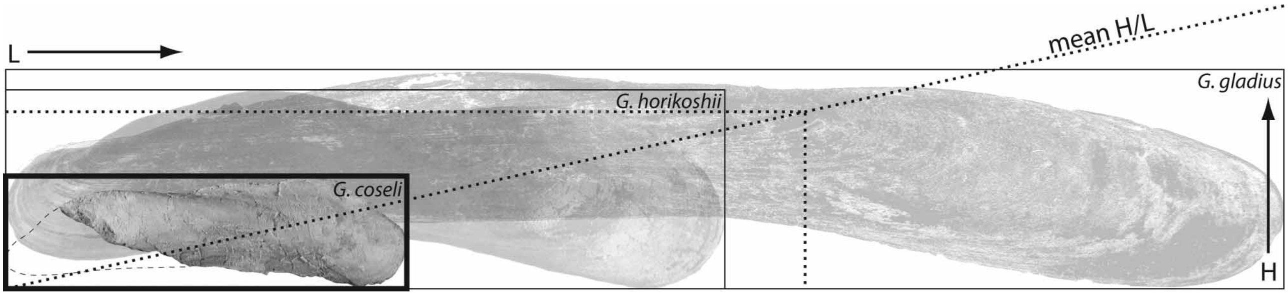

FIGURE 17. Diagram comparing relative maximum sizes reported* in modern species of the genus *Gigantidas* Cosel and B. Marshall, 2003 (thin-lined boxes), against the largest specimen** of *G. coseli* **sp. nov.** (specimen L4212). Mean maximum size (H = 43.7 mm, L = 197.7 mm) and H/L ratio (0.22) for genus shown by dashed lines. Faded background images are of largest specimen of both described modern species, *G. gladius* Cosel and B. Marshall, 2003 (H = 54.1 mm, L = 316.0 mm) and *G. horikoshii* Hashimoto and Yamane, 2005 (H = 49.1 mm, L = 177.8 mm). These holotype images are slightly distorted to fill the dimensions of the largest specimen of each species reported, modified from Cosel and Marshall (2003: fig. 25) and Hashimoto and Yamane (2005: fig. 8). H: shell height; L: shell length.
* Data acquired from published descriptions, where height values also are available for the purpose of this diagram. Cosel (unpublished data) has found a slightly greater maximum length for *G. horikoshii* (see Table 7).
** The potentially largest specimen of *G. coseli* **sp. nov.**, as inferred from a posterior portion (see description above), is ignored for the purpose of this diagram as the length cannot be accurately estimated.

Acknowledgements

We thank Rudo von Cosel (Muséum national d'Histoire naturelle, Département de Systématique et Evolution Taxonomie et Collections (Malacologie), Paris, France), Takami Nobuhara (Faculty of Education (Geology), University of Shizuoka, Shizuoka City, Japan), Luciana Génio (School of Earth and Environment, University of Leeds, Leeds, United Kingdom) and Margaret S. Morley (Auckland War Memorial Museum, Auckland, New Zealand) for providing unpublished data. We also extend appreciation to David A. Francis (Geological Research Limited, Lower Hutt, New Zealand), for field logistics and providing compiled New Zealand Fossil Record File (www.fred.org.nz) data for stratigraphic ages. Kareen Schnabel (Collection Manager, Marine Biodiversity and Biosecurity, National Institute of Water and Atmospheric Research Ltd., Wellington, New Zealand), provided comparative modern material. We are grateful to Neville Hudson (School of Environment, University of Auckland, Auckland, New Zealand) and John Simes (GNS Science, Lower Hutt, New Zealand) for assistance compiling materials data. Campbell S. Nelson, Steven Hood, Melissa Troup, Sarah Ewen, Stephanie Nyman and Susan Nyman (Department of Earth and Ocean Sciences, University of Waikato, Hamilton, New Zealand) provided field assistance. Two anonymous reviewers made comments that improved the manuscript. We also thank our translators, Ivana Alfaro (Italian literature), Hirotoshi Nishiwaki (Japanese literature), and Patrick Nadoll (German literature) for their work on our behalf. K.P.S. and K.A.C. acknowledge the School of Environment, University of Auckland, for its support and were funded by a research grant to K.A.C. from the Marsden Fund Council for government funding, administered by the Royal Society of New Zealand. Funding for C.T.S.L. was provided by the Royal Society.

References

Amano, K., Jenkins, R.G., Aikawa, M. & Nobuhara, T. (2010) A Miocene chemosynthetic community from the Ogaya Formation in Joetsu: evidence for depth-related ecologic control among fossil seep communities in the Japan Sea back-arc basin. *Palaeogeography, Palaeoclimatology, Palaeoecology*, 286, 164–170.

Amano, K. & Kanno, S. (2005) *Calyptogena* (Bivalvia: Vesicomyidae) from Neogene strata in the Joetsu District, Niigata Prefecture, Central Japan. *The Veliger*, 47, 202–212.

Ansell, J.H. & Bannister, S.C. (1996) Shallow morphology of the subducted Pacific plate along the Hikurangi margin, New Zealand. *Physics of the Earth and Planetary Interiors*, 93, 3–20.

Baco, A., Rowden, A.A., Levin, L.A., Smith, C.R. & Bowden, D. (2010) Initial characterization of cold seep faunal communities on the New Zealand margin. *Marine Geology*, 272, 251–259.

Ballance, P.F. (1976) Evolution of the Upper Cenozoic magmatic arc and plate boundary in northern New Zealand. *Earth and Planetary Science Letters*, 28, 356–370.

Barnes, P.M., Nicol, A. & Harrison, T. (2002) Late Cenozoic evolution and earthquake potential of an active listric thrust complex above the Hikurangi subduction zone, New Zealand. *The Geological Society of America Bulletin*, 114, 1379–1405.

Beu, A.G. & Maxwell, P.A. (1990) Cenozoic Mollusca of New Zealand. *New Zealand Geological Survey Paleontological Bulletin*, 58, 1–518.

Bohrmann, G., Heeschen, K., Jung, C., Weinrebe, W., Baranov, B., Cailleau, B., Heath, R., Huehnerbach, V., Hort, M., Masson, D. & Trummer, I. (2002) Widespread fluid expulsion along the seafloor of the Costa Rica convergent margin. *Terra Nova*, 14, 69–79.

Buonanni, P.F. (1681) *Ricreatione dell'occhio a della mente nell'osservation delle Chiocciole*. Il Varese, Rome, 384 pp.

Campbell, K.A. & Bottjer, D.J. (1993) Fossil cold seeps (Jurassic–Pliocene) along the convergent margin of western North America. *National Geographic Research and Exploration*, 9, 326–343.

Campbell, K.A., Francis, D.A., Collins, M., Gregory, M.R., Greinert, J. & Aharon, P. (2008) Hydrocarbon seep-carbonates of a Miocene forearc (East Coast Basin), North Island, New Zealand. *Sedimentary Geology*, 204, 83–105.

Campbell, K.A., Nelson, C.S., Alfaro, A.C., Boyd, S., Greinert, J., Nyman, S.L., Grosjean, E., Logan, G.A., Gregory, M.R., Cooke, S., Linke, P., Milloy, S. & Wallis, I. (2010) Geological imprint of methane seepage on the seabed and biota of the convergent Hikurangi Margin, New Zealand: box core and grab carbonate results. *Marine Geology*, 272, 285–306.

Carney, S.L., Formica, M.I., Divatia, H., Nelson, K., Fisher, C.R. & Schaeffer, S.W. (2006) Population structure of the mussel "*Bathymodiolus*" *childressi* from Gulf of Mexico hydrocarbon seeps. *Deep-Sea Research Part I: Oceanographic Research Papers*, 53, 1061–1072.

Collins, M. (1999) *A biometric and taxonomic study of Miocene-age, hydrocarbon-seep mussels from the East Coast of the North Island, New Zealand*. MSc thesis, University of Auckland, Auckland, 67 pp.

Cooper, R.A. (compiler) (2004) New Zealand Geological Timescale 2004/2 wallchart. *Institute of Geological and Nuclear Sciences information series 64*.

Cordes, E.E., Carney, S.L., Hourdez, S., Carney, R.S., Brooks, J.M. & Fisher, C.R. (2007) Cold seeps of the deep Gulf of Mexico: community structure and biogeographic comparisons to Atlantic equatorial belt seep communities. *Deep*

Sea Research Part I: Oceanographic Research Papers, 54, 637–653.

Cosel, R. von (2002) A new species of bathymodioline mussel (Mollusca, Bivalvia, Mytilidae) from Mauritania (West Africa), with comments on the genus *Bathymodiolus* Kenk & Wilson, 1985. *Zoosystema*, 24, 259–271.

Cosel, R. von (2008a) A new bathymodioline mussel (Bivalvia: Mytiloidea: Mytilidae: Bathymodiolinae) from vent sites near Kueishan Island, north east Taiwan. *The Raffles Bulletin of Zoology, Supplement No. 19*, 105–114.

Cosel, R. von (2008b) Bathymodioline mussels from hydrothermal vents and cold seeps – a history of an extraordinary discovery, and what is known today. *In*: Hourdez, S. & Sahling, H. (Eds.), *Report to ChEss on the workshop* Molecular phylogeny and taxonomy of vesciomyid (sic) and mytilid bivalves, *5th - 10th September, 2008*. *Station Biologique de Roscoff, Roscoff*, p. 14.

Cosel, R. von, Comtet, T. & Krylova, E.M. (1999) *Bathymodiolus* (Bivalvia: Mytilidae) from hydrothermal vents on the Azores Triple Junction and the Logatchev hydrothermal field, Mid-Atlantic Ridge. *The Veliger*, 42, 218–248.

Cosel, R. von & Janssen, R. (2008) Bathymodioline mussels of the *Bathymodiolus* (s. l.) *childressi* clade from methane seeps near Edison Seamount, New Ireland, Papua New Guinea (Bivalvia: Mytilidae). *Archiv für Molluskenkunde*, 137, 195–224.

Cosel, R. von & Marshall, B.A. (2003) Two new species of large mussels (Bivalvia: Mytilidae) from active submarine volcanoes and a cold seep off the eastern North Island of New Zealand, with description of a new genus. *The Nautilus*, 117, 31–46.

Cosel, R. von & Marshall, B.A. (2010) A new genus and species of large mussel (Mollusca: Bivalvia: Mytilidae) from the Kermadec Ridge. *Tuhinga*, 21, 59–73 [published 08/2010].

Cosel, R. von, Métivier, B. & Hashimoto, J. (1994) Three new species of *Bathymodiolus* (Bivalvia: Mytilidae) from hydrothermal vents in the Lau Basin and the North Fiji Basin, western Pacific, and the Snake Pit area, mid-Atlantic Ridge. *The Veliger*, 37, 374–392.

Cosel, R. von & Olu, K. (1998) Gigantism in Mytilidae. A new *Bathymodiolus* from cold seep areas on the Barbados accretionary Prism (sic). *Comptes Rendus de l'Académie des Sciences de Paris*, 321, 655–663.

Dautzenberg, P. (1927) Mollusques provenant des campagnes scientifiques du Prince Albert Ier de Monaco dans l'Ocean Altantique et dans le Golfe de Gascogne. *Résultats des Campagnes Scientifiques accomplies par Albert Ier*, 72, 1–400.

Distel, D., Baco, A.R., Chuang, E., Morrill, W., Cavanaugh, C. & Smith, C.R. (2000) Do mussels take wooden steps to deep-sea vents? *Nature*, 403, 725–726.

Férrusac, A.E.J.P.J.F.d'A. de (1822) *Tableaux systématiques des animaux mollusques. Classés en familles naturelles, dans lequels on a établi la concordance de tous les systèmes; suivis d'un prodrome général pour tous les mollusques terrestres ou fluviatiles, vivants ou fossiles*. Bertrand, Paris, 111 pp.

Fujita, Y., Matsumoto, H., Fujiwara, Y., Hashimoto, J., Galkin, S.V., Ueshima, R. & Miyazaki, J.-I. (2009) Phylogenetic relationships of deep-sea *Bathymodiolus* mussels to their mytilid relatives from sunken whale carcasses and wood. *Venus*, 67, 123–134.

Génio, L., Johnson, S.B., Vrijenhoek, R.C., Cunha, M.R., Tyler, P.A., Kiel, S. & Little, C.T.S. (2008) New record of "*Bathymodiolus*" *mauritanicus* Cosel 2002 from the Gulf of Cadiz (NE Atlantic) mud volcanoes. *Journal of Shellfish Research*, 27, 53–61.

Gill, F.L. (2005) *Fossil cold seep communities in the Caribbean region*. PhD thesis, University of Leeds, Leeds, 261 pp.

Gill, F.L., Harding, I.C., Little, C.T.S. & Todd, J.A. (2005) Palaeogene and Neogene cold seep communities in Barbados, Trinidad and Venezuela: an overview. *Palaeogeography, Palaeoclimatology, Palaeoecology*, 227, 191–209.

Goedert, J.L. & Campbell, K.A. (1995) An Early Oligocene chemosynthetic community from the Makah Formation, northwestern Olympic Peninsula, Washington. *The Veliger*, 38, 22–29.

Goedert, J.L. & Kaler, K.L. (1996) A new species of *Abyssochrysos* (Gastropoda: Loxonematoidea) from a Middle Eocene cold-seep carbonate in the Humptulips Formation, western Washington. *The Veliger*, 39, 65–70.

Goedert, J.L. & Squires, R.L. (1993) First Oligocene records of *Calyptogena* (Bivalvia: Vesicomyidae). *The Veliger*, 36, 72–77.

Goedert, J.L., Thiel, V., Schmale, O., Rau, W.W., Michaelis, W. & Peckmann, J. (2003) The Late Eocene 'Whiskey Creek' methane-seep deposit (western Washington State) Part I: geology, palaeontology, and molecular geobiology. *Facies*, 48, 223–240.

Gould, A.A. (1850) Shells from the United States Exploring Expedition. *Proceedings of the Boston Society of Natural History*, 3, 343–348.

Gustafson, R.G., Turner, R.D., Lutz, R.A. & Vrijenhoek, R.C. (1998) A new genus and five new species of mussels (Bivalvia, Mytilidae) from deep-sea sulfide/hydrocarbon seeps in the Gulf of Mexico. *Malacologia*, 40, 63–112.

Han, X., Suess, E., Sahling, H. & Wallmann, K. (2004) Fluid venting activity on the Costa Rica margin: new results from authigenic carbonates. *International Journal of Earth Sciences*, 93, 596–611.

Hashimoto, J. (2001) A new species of *Bathymodiolus* (Bivalvia: Mytilidae) from hydrothermal vent communities in the Indian Ocean. *Venus*, 60, 141–149.

Hashimoto, J. & Furuta, M. (2007) A new species of *Bathymodiolus* (Bivalvia: Mytilidae) from hydrothermal vent communities in the Manus Basin, Papua New Guinea. *Venus*, 66, 57–68.

Hashimoto, J. & Horikoshi, M. (1989) A burrowing species of "*Bathymodiolus*". *Deep-Sea Newsletter*, 15, 32–34.

Hashimoto, J. & Okutani, T. (1994) Four new mytilid mussels associated with deepsea (sic) chemosynthetic communities around Japan. *Venus*, 53, 61–83.

Hashimoto, J. & Yamane, T. (2005) A new species of *Gigantidas* (Bivalvia: Mytilidae) from a vent site on the Kaikata Seamount southwest of the Ogasawara (Bonin) Islands, southern Japan. *Venus*, 64, 1–10.

Hayward, B.W. (1978) FRED :: Sample Detail for Y18/f0013. Available from http://www.fred.org.nz/detail.jsp?ID=76618 (accessed 1 March 2010).

Hayward, B.W. (1986) A guide to paleoenvironmental assessment using New Zealand Cenozoic forminiferal (sic) faunas. *New Zealand Geological Survey Report Pal 109*, 1–73.

Iwasaki, H., Kyuno, A., Shintaku, M., Fujita, Y., Fujiwara, Y., Fujikura, K., Hashimoto, J., Oliveira Martins, L. de, Gebruk, A. & Miyazaki, J.-I. (2006) Evolutionary relationships of deep-sea mussels inferred by mitochondrial DNA sequences. *Marine Biology*, 149, 1111–1122.

Jones, W.J. & Vrijenhoek, R.C. (2006) Evolutionary relationships within the *"Bathymodiolus" childressi* group. *Cahiers de Biologie Marine*, 47, 403–407.

Jones, W.J., Won, Y.-J., Maas, P.A., Smith, P.J., Lutz, R.A. & Vrijenhoek, R.C. (2006) Evolution of habitat use by deep-sea mussels. *Marine Biology*, 148, 841–851.

Keen, A.M. (1958) *Marine shells of tropical West America.* Stanford University Press, Stanford, 624 pp.

Kenk, V.C. & Wilson, B.R. (1985) A new mussel (Bivalvia, Mytilidae) from hydrothermal vents in the Galapagos Rift zone. *Malacologia*, 26, 253–271.

Kennish, M.J., Antonieto, S.T. & Lutz, R.A. (1998) Shell microstructure of mytilids (Bivalvia) from deep-sea hydrothermal vent and cold-water sulfide/methane seep environments. *The Nautilus*, 112, 84–89.

Kiel, S. (2006) New records and species of molluscs from Tertiary cold-seep carbonates in Washington State, USA. *Journal of Paleontology*, 80, 121–137.

Kiel, S., Campbell, K.A. & Gailliard, C. (2010) New and little known mollusks from ancient chemosynthetic environments. *Zootaxa*, 2390, 26–48.

Krylova, E.M. & Janssen, R. (2006) Vesicomyidae from Edison Seamount (south-west Pacific: Papua New Guinea: New Ireland fore-arc basin). *Archiv für Molluskenkunde*, 135, 231–261.

Kuroda, T. (1931) Fossil Mollusca from Shinano. *In*: Honma, F. (Ed.) *Geology of Central Shinano, Part 1* (in Japanese). Kokin-Shoin Publication Company Limited, Tokyo, pp. 1–90.

Lewis, K.B. & Marshall, B.A. (1996) Seep faunas and other indicators of methane-rich dewatering on New Zealand convergent margins. *New Zealand Journal of Geology and Geophysics*, 39, 181–200.

Linnaeus, C. (1758) *Systema naturae per regna tria naturae, secundum classes, ordines, genera, species, cum characteribus, differentiis, synonymis, locis. Editio decima.* Laurentius Salvius, Stockholm, 824 pp.

Lonsdale, P.F. (1977) Clustering of suspension-feeding macrobenthos near abyssal hydrothermal vents at oceanic spreading centers. *Deep-Sea Research*, 24, 857–863.

Majima, R., Nobuhara, T. & Kitazaki, T. (2005) Review of fossil chemosynthetic assemblages in Japan. *Palaeogeography, Palaeoclimatology, Palaeoecology*, 227, 86–123.

Marwick, J. (1931) The Tertiary Mollusca of the Gisborne district. *New Zealand Geological Survey Palaeontological Bulletin*, 13, 1–177.

Mau, S., Sahling, H., Rehder, G., Suess, E., Linke, P. & Soeding, E. (2006) Estimates of methane output from mud extrusions at the erosive convergent margin off Costa Rica. *Marine Geology*, 225, 129–144.

McKiness, Z.P. & Cavanaugh, C.M. (2005) The ubiquitous mussel: *Bathymodiolus* aff. *brevior* symbiosis at the Central Indian Ridge hydrothermal vents. *Marine Ecology Progress Series*, 295, 183–190.

McKiness, Z.P., McMullin, E.R., Fisher, C.R. & Cavanaugh, C.M. (2005) A new bathymodioline mussel symbiosis at the Juan de Fuca hydrothermal vents. *Marine Biology*, 148, 109–116.

Miyazaki, J.-I., Shintaku, M., Kyuno, A., Fujiwara, Y., Hashimoto, J. & Iwasaki, H. (2004) Phylogenetic relationships of deep-sea mussels of the genus *Bathymodiolus* (Bivalvia: Mytilidae). *Marine Biology*, 144, 527–535.

Moroni, M.A. (1966) Malacofauna di “Calcare a Lucine” di S. Sofia – Forlì. *Palaeontographia Italica*, 60, 69–87.

Nobuhara, T. (2003) Cold seep carbonate mounds with *Vesicomya* (*Calyptogena*) *kawamurai* (Bivalvia: Vesicomyidae) in slope-mud facies of the Pliocene forearc basin of the Sagara-Kakegawa area, central Japan. *Paleontological Research*, 7, 313–328.

Nobuhara, T., Imaizumi, I., Kaneko, T., Koike, H., Narita, K. & Amano, K. (2008) Mode of occurrence and taxonomical re-examination of modioliform bivalves from the lower Middle Miocene cold-seep carbonates in the Bessho Formation, Nagano Prefecture, central Japan (in Japanese). *Venus*, 67, 102.

Okutani, T., Fujikura, K. & Sasaki, T. (2004) Two new species of *Bathymodiolus* (Bivalvia: Mytilidae) from methane seeps on the Kuroshima Knoll off the Yaeyama Islands, southwestern Japan. *Venus*, 62, 97–110.

Olu-Le Roy, K., Cosel, R. von, Hourdez, S., Carney, S.L. & Jollivet, D. (2007) Amphi-Atlantic cold-seep *Bathymodiolus* species complexes across the equatorial belt. *Deep-Sea Research Part I: Oceanographic Research Papers*, 54, 1890–1911.

Rad, U. von, Berner, U., Delisle, G., Doose-Rolinski, H., Fechner, N., Linke, P., Lückge, A., Roeser, H.A., Schmaljohann, R., Wiedicke, M. & SONNE 122/130 Scientific Parties (2000) Gas and fluid venting at the Makran accretionary wedge off Pakistan. *Geo-Marine Letters*, 20, 10–19.

Rafinesque, C.S. (1815) *Analyse de la nature ou tableau de l'univers et des corps organisés*. Barravechia, Palermo, 224 pp.

Rait, G., Chanier, F. & Waters, D.W. (1991) Landward and seaward-directed thrusting accompanying the onset of subduction beneath New Zealand. *Geology*, 19, 230–233.

Sacco, F. (1898) *I molluschi dei terreni terziarii del Piemonte e della Liguria. Parte XXV. (Spondylidae, Radulidae, Aviculidae, Vulsellidae, Pernidae, Pinnidae, Mytilidae, Dreissensiidae)*. Clausen, Torino, 77 pp.

Saether, K.P., Little, C.T.S. & Campbell, K.A. (2010) A new fossil provannid gastropod from Miocene hydrocarbon seep deposits, East Coast Basin, North Island, New Zealand. *Acta Palaeontologica Polonica*, 55, doi: 10.4202/app.2009.1112.

Samadi, S., Quémére, E., Lorion, J., Tillier, A., Cosel, R. von, Lopez, P., Cruaud, C., Couloux, A. & Boisselier-Dubayle, M.-C. (2007) Molecular phylogeny in mytilids supports the wooden steps to deep-sea vents hypothesis. *Comptes Rendus Biologies*, 330, 446–456.

Scott, G.H. (1985) FRED :: Sample Detail for Y16/f0512. Available from http://www.fred.org.nz/detail.jsp?ID=76618 (accessed 1 March 2010).

Smith, P.J., McVeagh, S.M., Won, Y. & Vrijenhoek, R.C. (2004) Genetic heterogeneity among New Zealand species of hydrothermal vent mussels (Mytilidae: *Bathymodiolus*). *Marine Biology*, 144, 537–545.

Squires, R.L. & Goedert, J.L. (1991) New Late Eocene mollusks from localized limestone deposits formed by subduction-related methane seeps, southwestern Washington. *Journal of Paleontology*, 65, 412–416.

Squires, R.L. & Goedert, J.L. (1995) An extant species of *Leptochiton* (Mollusca: Polyplacophora) in Eocene and Oligocene cold-seep limestones, Olympic Peninsula, Washington. *The Veliger*, 38, 47–53.

Stanley, S.M. (1973) An explanation for Cope's rule. *Evolution*, 27, 1–26.

Tanaka, K. (1959) Molluscan fossils from central Shinano, Nagano Prefecture, Japan (Part 1). *Journal of the Faculty of Science, Shinshu University*, 8, 115–133.

Taviani, M. (1994) The "calcari a *Lucina*" macrofauna reconsidered: deep-sea faunal oases from Miocene-age cold vents in the Romagna Apennine, Italy. *Geo-Marine Letters*, 14, 185–191.

Van Dover, C.L., Aharon, P., Bernhard, J.M., Caylor, E., Doerries, M.B., Flickinger, W., Gilhooly, W.P., Goffredi, S.K., Knick, K.E., Macko, S.A., Rapoport, S., Raulfs, E.C., Ruppel, C.D., Salerno, J.L., Seitz, R.D., Sen Gupta, B.K., Shank, T.M., Turnipseed, M. & Vrijenhoek, R.C. (2003) Blake Ridge methane seeps: characterization of a soft-sediment, chemosynthetically based ecosystem. *Deep-Sea Research Part I: Oceanographic Research Papers*, 50, 281–300.

Van Dover, C.L., Humphris, S., Fornari, D.J., Cavanaugh, C.M., Collier, R., Goffredi, S.K., Hashimoto, J., Lilley, M.D., Reysenbach, A.L., Shank, T.M., Von Damm, K.L., Banta, A., Gallant, R.M., Gotz, D., Green, D., Hall, J., Harmer, T.L., Hurtado, L.A., Johnson, P., McKiness, Z.P., Meredith, C., Olson, E., Pan, I.L., Turnipseed, M., Won, Y.-J., Young, C.R., III & Vrijenhoek, R.C. (2001) Biogeography and ecological setting of Indian Ocean hydrothermal vents. *Science*, 294, 818–823.

Won, Y.-J., Jones, W.J. & Vrijenhoek, R.C. (2008) Absence of cospeciation between deep-sea mytilids and their thiotrophic endosymbionts. *Journal of Shellfish Research*, 27, 129–138.

Won, Y.-J., Young, C.R., III, Lutz, R.A. & Vrijenhoek, R.C. (2003) Dispersal barriers and isolation among deep-sea mussel populations (Mytilidae: *Bathymodiolus*) from eastern Pacific hydrothermal vents. *Molecular Ecology*, 12, 169–184.

Appendix I. Supplementary data

Measurement and specimen data for non-type and non-figured material used in this study.

Bathymodiolus heretaunga **sp. nov.**

Collection No.	Locality No.	Specimen No.	A	H	L	H/L	U
AU 15833	Y16/f1048	L4115	1.4	9.4	20.2	0.47	7%
AU 15833	Y16/f1048	L4185	1.6	8.9	16.7	0.53	10%
AU 15833	Y16/f1048	L4127	1.4	8.1	15.7	0.52	9%
AU 15833	Y16/f1048	L4128	0.3	3.7	6.5	0.57	5%
GS 13949	Y16/f0566	TM8707	4.0	20.3	36.6	0.55	11%
GS 13949	Y16/f0566	TM8708	0.8	7.0	13.6	0.51	6%
GS 13949	Y16/f0566	TM8709	2.6	16.2	32.8	0.49	8%
GS 13949	Y16/f0566	TM8710	1.5	12.7	26.7	0.48	6%
GS 13949	Y16/f0566	TM8711	1.4	7.0	16.0	0.44	9%
GS 13949	Y16/f0566	TM8712	1.4	10.2	20.9	0.49	7%
GS 13949	Y16/f0566	TM8713	2.7	13.0	25.1	0.52	11%
GS 13949	Y16/f0566	TM8714	1.7	14.0	29.7	0.47	6%
GS 13949	Y16/f0566	TM8715	2.4	15.6	31.8	0.49	8%
AU 19617	Y16/f1032	L4517	1.7	14.2	32.0	0.44	5%
AU 19617	Y16/f1032	L4518	2.6	18.3	43.6	0.42	6%
AU 19617	Y16/f1032	L4519	4.5	14.3	34.1	0.42	13%
AU 19617	Y16/f1032	L4520	2.2	14.0	33.1	0.42	7%
AU 19617	Y16/f1032	L4521	1.9	13.1	32.2	0.41	6%
AU 19617	Y16/f1032	L4522	2.3	11.3	23.7	0.48	10%
GS 14041	Y16/f0575	TM8716	3.7	21.3	41.1	0.52	9%
AU19659	Y16/f1046	L4523	5.7	21.0	46.5	0.45	12%
AU 15857	Y16/f1049	L4107	2.8	27.8	55.6	0.50	5%
AU 15857	Y16/f1049	L4184	1.0	5.7	13.0	0.44	8%
AU 15857	Y16/f1049	L4187	1.6	16.8	35.5	0.47	5%
AU19661	Y16/f1051	L4524	4.7	17.3	35.6	0.49	13%
AU19662	Y16/f1052	L4525	2.8	11.2	24.9	0.45	11%
AU19662	Y16/f1052	L4526	5.2	15.8	36.3	0.44	14%
AU 19618	Y16/f1033	L4570	3.6	19.4	37.2	0.52	10%
AU 15844	Y16/f1054	L4129	1.8	9.7	19.1	0.51	9%
GS 14044	Y16/f0580	Unnumbered	2.1	15.3	33.1	0.46	6%
GS 14044	Y16/f0580	TM8718	1.8	14.0	31.0	0.45	6%
GS 14044	Y16/f0580	TM8720	2.5	14.0	28.9	0.48	9%
GS 14044	Y16/f0580	Unnumbered	2.0	11.0	21.3	0.52	9%
GS 14044	Y16/f0580	Unnumbered	1.0	5.5	9.7	0.57	10%
GS 14044	Y16/f0580	TM8721	1.0	6.2	12.1	0.51	8%
GS 14044	Y16/f0580	TM8722	0.9	6.4	11.8	0.54	8%
GS 14044	Y16/f0580	TM8723	2.5	11.9	24.5	0.49	10%
GS 14044	Y16/f0580	TM8725	2.3	10.6	22.1	0.48	10%

continued next page

continued.

Collection No.	Locality No.	Specimen No.	A	H	L	H/L	U
GS 14044	Y16/f0580	Unnumbered	1.8	8.1	17.8	0.46	10%
AU 19619	Y16/f1034	L4527	4.2	17.1	31.4	0.54	13%
AU 19619	Y16/f1034	L4528	4.6	16.2	32.7	0.50	14%
AU 19619	Y16/f1034	L4529	2.6	15.4	31.4	0.49	8%
AU 19619	Y16/f1034	L4530	3.1	18.7	37.1	0.50	8%
GS 14184	Y16/f0642	Unnumbered	2.6	15.5	31.6	0.49	8%
GS 14184	Y16/f0642	TM8726	2.6	15.8	31.4	0.50	8%
GS 14184	Y16/f0642	TM8727	3.0	14.4	27.5	0.52	11%
GS 14184	Y16/f0642	TM8729	3.1	18.7	38.3	0.49	8%
GS 14183	Y16/f0641	TM8730	1.1	11.0	22.7	0.48	5%
GS 14184	Y16/f0642	TM8731	4.2	16.7	30.7	0.54	14%
AU 15854	Y16/f1028	L4085	3.0	21.3	39.5	0.54	8%
AU 15854	Y16/f1028	L4090	3.3	19.9	40.1	0.50	8%
AU 15854	Y16/f1028	L4105	5.1	21.4	44.4	0.48	11%
AU 15854	Y16/f1028	L4202	3.2	16.7	36.0	0.46	9%
AU 15834	Y16/f1029	L4152	1.7	12.9	25.3	0.51	7%
AU 15834	Y16/f1029	L4153	1.8	11.1	19.8	0.56	9%
AU 15847	Y16/f1036	L4064	1.7	18.2	32.2	0.57	5%
AU 15847	Y16/f1036	L4065	3.3	17.1	37.5	0.46	9%
AU 15847	Y16/f1036	L4067	1.7	16.8	29.3	0.57	6%
AU 15847	Y16/f1036	L4159	3.7	17.5	36.3	0.48	10%
AU 15847	Y16/f1036	L4161	3.1	14.5	31.8	0.46	10%
AU 15847	Y16/f1036	L4168	3.1	13.8	29.5	0.47	11%
AU 15847	Y16/f1036	L4077	2.2	17.0	33.5	0.51	7%
AU 15847	Y16/f1036	L4169	3.4	16.3	34.4	0.47	10%
AU 15847	Y16/f1036	L4170	2.1	17.7	35.6	0.50	6%
AU 15847	Y16/f1036	L4082	1.4	11.8	20.9	0.56	7%
AU 15847	Y16/f1036	L4091	3.6	21.2	45.4	0.47	8%
AU 15847	Y16/f1036	L4177	3.4	18.9	39.1	0.48	9%
AU 15847	Y16/f1036	L4117	3.2	19.5	36.7	0.53	9%
AU 15847	Y16/f1036	L4182	2.3	17.9	36.9	0.49	6%
AU 15847	Y16/f1036	L4183	4.4	21.1	48.4	0.44	9%
AU 15847	Y16/f1036	L4531	4.6	20.4	40.5	0.50	11%
AU 15847	Y16/f1036	L4532	3.7	15.4	33.3	0.46	11%
AU 15847	Y16/f1036	L4533	4.7	23.3	43.8	0.53	11%
AU 15847	Y16/f1036	L4534	4.0	24.1	45.0	0.54	9%
AU 15847	Y16/f1036	L4535	2.2	13.9	26.4	0.53	8%
AU 15847	Y16/f1036	L4536	1.7	8.7	18.8	0.46	9%
AU 15845	Y16/f1036	L4086	3.1	20.3	37.2	0.55	8%
AU 15845	Y16/f1036	L4092	3.4	19.2	40.2	0.48	8%
AU 15845	Y16/f1036	L4172	2.5	21.4	40.6	0.53	6%

continued next page

continued.

Collection No.	Locality No.	Specimen No.	A	H	L	H/L	U
AU 15845	Y16/f1036	L4093	1.8	14.0	26.5	0.53	7%
AU 15845	Y16/f1036	L4094	3.0	13.5	28.6	0.47	10%
AU 15845	Y16/f1036	L4095	1.6	16.9	30.7	0.55	5%
AU 15845	Y16/f1036	L4096	1.3	13.6	25.2	0.54	5%
AU 15845	Y16/f1036	L4173	2.6	18.9	39.4	0.48	7%
AU 15845	Y16/f1036	L4174	1.7	12.1	25.7	0.47	7%
AU 15845	Y16/f1036	L4098	2.6	20.7	38.1	0.54	7%
AU 15845	Y16/f1036	L4176	2.3	19.5	34.5	0.57	7%
AU 15845	Y16/f1036	L4102	2.2	15.7	28.4	0.55	8%
AU 15845	Y16/f1036	L4136	3.7	22.5	43.3	0.52	9%
AU 15846	Y16/f1036	L4087	1.6	11.7	21.7	0.54	7%
AU 15846	Y16/f1036	L4108	4.3	18.0	36.6	0.49	12%
AU 15846	Y16/f1036	L4110	2.0	17.4	34.2	0.51	6%
AU 15846	Y16/f1036	L4111	1.6	9.9	17.3	0.57	9%
AU 15846	Y16/f1036	L4134	3.2	18.6	33.8	0.55	9%
AU 15849	Y16/f1037	L4074	2.5	14.0	30.2	0.46	8%
AU 15849	Y16/f1037	L4164	1.5	11.9	26.1	0.46	6%
AU 15849	Y16/f1037	L4181	2.4	13.7	27.3	0.50	9%
AU 15849	Y16/f1037	L4125	4.0	16.4	36.2	0.45	11%
AU 15849	Y16/f1037	L4186	2.5	14.6	30.8	0.47	8%
AU 15849	Y16/f1037	L4189	2.9	17.3	35.8	0.48	8%
AU 15849	Y16/f1037	Unnumbered	3.5	13.3	29.8	0.45	12%
AU 15849	Y16/f1037	L4537	4.3	15.8	31.5	0.50	14%
AU 15849	Y16/f1037	L4538	2.5	10.7	20.7	0.52	12%
AU 15849	Y16/f1037	L4539	3.9	13.7	31.1	0.44	13%
AU 19621	Y16/f1038	L4151	4.2	16.3	32.0	0.51	13%
AU 15853	Y16/f1039	L4083	2.1	16.8	35.5	0.47	6%
AU 15853	Y16/f1039	L4089	2.0	21.8	39.2	0.56	5%
AU 19609	Y16/f1030	L4540	3.0	11.9	21.6	0.55	14%
AU 19609	Y16/f1030	L4541	1.6	11.9	21.0	0.57	8%
AU 19609	Y16/f1030	L4542	1.6	8.1	14.8	0.55	11%
AU 15851	Y16/f1040	L4165	2.7	16.8	34.1	0.49	8%
AU 15851	Y16/f1040	L4167	2.5	9.1	20.7	0.44	12%
AU 15850	Y16/f1040	L4075	2.7	12.8	24.1	0.53	11%
AU 15850	Y16/f1040	L4076	1.7	12.0	21.9	0.55	8%
AU 15856	Y16/f1041	L4106	3.2	25.7	48.5	0.53	7%
AU 15856	Y16/f1041	L4197	3.5	14.8	30.1	0.49	12%
AU 15856	Y16/f1041	L4139	5.0	26.7	46.8	0.57	11%
AU 15856	Y16/f1041	L4140	1.0	8.9	16.3	0.55	6%
AU 15856	Y16/f1041	L4199	2.6	14.7	31.4	0.47	8%
AU 19622	Y16/f1042	L4543	4.2	21.1	40.3	0.52	10%

continued next page

continued.

Collection No.	Locality No.	Specimen No.	A	H	L	H/L	U
AU 19622	Y16/f1042	L4544	2.6	14.3	27.3	0.52	10%
AU 15848	Y16/f1043	L4072	3.5	19.5	38.1	0.51	9%
AU 15848	Y16/f1043	L4073	2.7	18.3	33.0	0.55	8%
AU 15848	Y16/f1043	L4180	4.1	16.6	32.7	0.51	13%
AU 19623	Y16/f1044	L4545	3.4	17.9	36.2	0.49	9%
GS 13850	Y16/f0539	TM8732	5.3	29.8	62.7	0.48	8%
GS 13850	Y16/f0539	Unnumbered	4.5	30.4	68.4	0.44	7%
GS 13850	Y16/f0539	TM8735	5.8	29.0	64.0	0.45	9%
GS 13850	Y16/f0539	TM8736	4.3	25.0	55.9	0.45	8%
GS 13850	Y16/f0539	TM8737	6.4	24.7	56.2	0.44	11%
GS 13850	Y16/f0539	TM8738	5.2	28.1	60.6	0.46	9%
GS 13850	Y16/f0539	Unnumbered	5.3	22.7	52.3	0.43	10%
AU 15836	Y16/f1055	L4123	0.7	6.3	11.6	0.54	6%
AU 15836	Y16/f1055	L4546	5.3	19.9	39.9	0.50	13%
GS 14041	Y16/f0575	TM8739	5.3	25.0	54.3	0.46	10%
GS 14041	Y16/f0575	Unnumbered	5.2	18.8	38.0	0.49	14%
GS 14041	Y16/f0575	TM8740	3.0	25.4	52.2	0.49	6%
GS 14041	Y16/f0575	TM8741	3.7	20.2	41.4	0.49	9%
GS 14041	Y16/f0575	TM8742	3.4	24.3	54.7	0.44	6%
GS 14041	Y16/f0575	TM8743	2.6	13.2	27.3	0.48	10%
GS 14041	Y16/f0575	TM8744	2.5	21.9	50.2	0.44	5%
GS 14041	Y16/f0575	Unnumbered	5.4	20.0	37.5	0.53	14%
GS 14041	Y16/f0575	Unnumbered	2.7	19.0	41.8	0.45	6%
AU 15839	Y16/f1056	L4116	1.7	13.7	25.2	0.54	7%
AU 15840	Y16/f1056	L4190	5.3	25.8	52.6	0.49	10%
AU 15840	Y16/f1056	L4192	3.4	20.3	46.5	0.44	7%
AU 15840	Y16/f1056	L4196	2.6	20.0	47.2	0.42	6%
AU 15840	Y16/f1056	L4137	3.4	14.0	27.8	0.50	12%
AU 15841	Y16/f1056	L4131	3.5	14.4	25.8	0.56	14%
AU 15841	Y16/f1056	L4193	5.7	26.8	54.7	0.49	10%
AU 15841	Y16/f1056	L4194	5.6	22.6	48.4	0.47	12%
AU 15841	Y16/f1056	L4133	6.4	25.7	55.6	0.46	12%
AU 15841	Y16/f1056	L4195	4.5	26.4	57.2	0.46	8%
AU 15841	Y16/f1056	L4143	3.2	15.5	29.8	0.52	11%
AU 15843	Y16/f1056	L4061	1.3	11.1	21.5	0.52	6%
AU 15843	Y16/f1056	L4155	4.2	19.2	41.4	0.46	10%
AU 15843	Y16/f1056	L4156	5.2	20.2	48.4	0.42	11%
AU 15843	Y16/f1056	L4062	1.3	9.0	17.2	0.52	8%
AU 15843	Y16/f1056	L4063	3.4	29.4	57.7	0.51	6%
AU 15843	Y16/f1056	L4157	3.3	18.7	33.9	0.55	10%
AU 15843	Y16/f1056	L4158	5.1	18.5	42.4	0.44	12%

continued next page

continued.

Collection No.	Locality No.	Specimen No.	A	H	L	H/L	U
AU 15843	Y16/f1056	L4162	3.1	16.2	36.6	0.44	8%
AU 15843	Y16/f1056	L4163	6.7	22.8	49.4	0.46	14%
AU 15843	Y16/f1056	L4113	1.4	10.6	20.0	0.53	7%
AU 15843	Y16/f1056	L4114	0.7	4.3	7.5	0.57	9%
AU 15843	Y16/f1056	L4132	4.2	16.3	30.4	0.54	14%
AU 15843	Y16/f1056	L4141	3.5	14.1	27.1	0.52	13%
AU 15843	Y16/f1056	L4142	1.7	9.0	16.4	0.55	10%
AU 15843	Y16/f1056	L4144	4.3	22.0	43.9	0.50	10%
AU 15843	Y16/f1056	L4146	6.3	23.1	51.7	0.45	12%
AU 15843	Y16/f1056	L4147	7.0	28.0	61.7	0.45	11%
AU 15843	Y16/f1056	L4148	4.7	22.9	45.4	0.50	10%
AU 15843	Y16/f1056	L4149	6.6	24.1	46.2	0.52	14%
AU 15843	Y16/f1056	L4154	4.6	25.9	52.8	0.49	9%
AU 19663	U23/f0266	L4547	1.2	7.6	17.8	0.43	7%
AU 19663	U23/f0266	L4548	1.6	11.6	26.5	0.44	6%
AU 19664	U23/f0266	L4549	3.1	11.9	24.4	0.49	13%
AU 19664	U23/f0266	L4550	2.2	11.2	24.3	0.46	9%
AU 19664	U23/f0266	L4551	2.7	13.6	25.5	0.53	11%
AU 19664	U23/f0266	L4571	2.7	15.2	29.8	0.51	9%
AU 19664	U23/f0266	L4552	3.2	11.4	25.4	0.45	13%
AU 19664	U23/f0266	L4553	1.8	13.4	31.8	0.42	6%
AU 19664	U23/f0266	L4572	3.4	11.9	29.3	0.41	12%
AU 19664	U23/f0266	L4573	2.4	15.0	31.8	0.47	8%
AU 19664	U23/f0266	L4574	1.9	11.7	25.6	0.46	7%
AU 19664	U23/f0266	Unnumbered	2.0	12.3	27.4	0.45	7%
AU 19664	U23/f0266	L4554	1.4	8.3	20.2	0.41	7%
AU 19664	U23/f0266	L4555	2.0	15.0	28.5	0.53	7%
AU 19664	U23/f0266	L4557	3.1	15.0	34.7	0.43	9%
GS 2042	U23/f7464	TM8746	0.9	9.3	19.1	0.49	5%
GS 2042	U23/f7464	TM8747	2.0	14.3	32.4	0.44	6%
GS 2042	U23/f7464	Unnumbered	2.4	18.0	42.0	0.43	6%
GS 686	Z16/f7491	TM8748	4.4	19.3	40.9	0.47	11%
AU 19620	Z16/f0075	L4558	4.2	15.9	31.0	0.51	14%

Gigantidas coseli **sp. nov.**

Collection No.	Locality No.	Specimen No.	A	H	L	H/L	U
AU 19618	Y16/f1033	L4564	9.7	22.0	76.7	0.29	13%
AU 19618	Y16/f1033	L4565	---	20.8	77.6	0.27	---
AU 19618	Y16/f1033	L4566	8.9	20.0	64.2	0.31	14%
AU 15844	Y16/f1054	L4208	10.3	20.1	85.8	0.23	12%
AU 15844	Y16/f1054	L4210	11.4	21.9	92.3	0.24	12%
AU 15844	Y16/f1054	L4206	6.3	28.7	84.2	0.34	7%
AU 15844	Y16/f1054	L4207	4.7	23.3	83.3	0.28	6%
AU 15844	Y16/f1054	L4567	---	21.6	73.3	0.29	---
AU 15844	Y16/f1054	L4212	---	27.8	99.2	0.28	---
AU 19660	Y16/f1054	L4568	---	16.2	54.8	0.30	---
GS 14044	Y16/f0580	TM8751	6.4	10.9	28.1	0.39	23%
AU19658	Y16/f1047	L4569	10.5	21.8	78.6	0.28	13%
AU 15846	Y16/f1036	L4205	1.7	8.2	24.6	0.33	7%
AU 15845	Y16/f1036	L4214	8.6	15.6	62.9	0.25	14%
AU 19648	Y16/f1043	Unnumbered	5.6	20.1	61.2	0.33	9%
GS 14242	Y18/f0372	TM8752	9.7	22.7	79.6	0.29	12%
GS 14242	Y18/f0372	TM8753	11.8	25.5	93.0	0.27	13%